Errors recruit both cognitive and emotional monitoring systems: simultaneous intracranial recordings in the dorsal anterior cingulate gyrus and amygdala combined with fMRI

Gilles Pourtois[1,2], Roland Vocat[2], Karim N'Diaye[2,3], Laurent Spinelli[4,5],

Margitta Seeck[4,5], & Patrik Vuilleumier[2,3]

(1) Department of Experimental Clinical and Health Psychology, Ghent University, Belgium

(2) Laboratory for Behavioral Neurology & Imaging of Cognition, Department of Neuroscience & Clinic of Neurology, University of Geneva, Geneva, Switzerland

(3) Swiss Center for Affective Sciences, University of Geneva, Geneva, Switzerland

(4) Pre-surgical Epilepsy Evaluation Unit, Clinic of Neurology, University Hospital, Geneva, Switzerland

(5) Functional Brain Mapping Laboratory, Department of Neuroscience, University of Geneva, Geneva, Switzerland

Correspondence:

Gilles Pourtois

Department of Experimental clinical and health psychology

Ghent University

Henri Dunantlaan 2

9000 Gent

Belgium

Phone: +32 9 264 9144

Email: gilles.pourtois@ugent.be

Abstract

We studied error monitoring in a human patient with unique implantation of depth electrodes in both the left dorsal cingulate gyrus and medial temporal lobe prior to surgery. The patient performed a speeded go/nogo task and made a substantial number of commission errors (false alarms). As predicted, intracranial Local Field Potentials (iLFPs) in dorsal anterior cingulate indexed the detection of errors, showing an early differential activity around motor execution for false alarms, relative to correct responses (either hits or correct inhibitions). More surprisingly, we found that the left amygdala also participated to error monitoring (although no emotional stimuli were used), but with a very different neurophysiological profile as compared with the dorsal cingulate cortex. Amygdala iLFPs showed a precise and reproducible temporal unfolding, characterized by an early monophasic response for correct hits around motor execution, which was delayed by ~300 ms for errors (even though actual RTs were almost identical in these two conditions). Moreover, time-frequency analyses demonstrated a reliable and transient coupling in the theta band around motor execution between these two distant regions. Additional fMRI investigation in the same patient confirmed a differential involvement of the dorsal cingulate cortex vs. amygdala in error monitoring during this go/nogo task. Finally, these intracranial results for the left amygdala were replicated in a second patient with intracranial electrodes in the right amygdala. Altogether, these results suggest that the amygdala may register the motivational significance of motor actions on a trial-by-trial basis, while the dorsal anterior cingulate cortex may provide signals concerning failures of cognitive control and behavioral adjustment. More generally, these data shed new light on neural mechanisms underlying self monitoring by showing that even "simple" motor actions recruit not only executive cognitive processes (in dorsal cingulate) but also affective processes (in amygdala).

Keywords: false alarms; commission errors; error detection; cognitive control; emotional effects; dorsal anterior cingulate cortex; amygdala; epilepsy; human intracranial EEG; fMRI.

Introduction

Error detection is an essential cognitive function for adaptive and flexible behaviors (Rabbitt, 1966; Gratton, Coles, & Donchin, 1992; Ullsperger & von Cramon, 2004). Error detection allows a rapid adjustment of actions based on their perceived outcome, and may therefore play a critical role in reinforcement learning (Holroyd & Coles, 2002; Cohen & Ranganath, 2007). In this model, errors modify the strength of stimulus-response mappings, thereby altering and improving subsequent actions in an appropriate manner. Error detection has been shown, by electrophysiology (Dehaene, Posner, & Tucker, 1994; Falkenstein, Hoormann, Christ, & Hohnsbein, 2000; Gehring & Fencsik, 2001; van Veen & Carter, 2002, 2006; Debener et al., 2005), lesion (Swick & Turken, 2002; Cohen, Ridderinkhof, Haupt, Elger, & Fell, 2008 but see Fellows & Farah, 2005), functional neuroimaging (Carter et al., 1998; Ullsperger & von Cramon, 2001; Brown & Braver, 2005; Stevens, Kiehl, Pearlson, & Calhoun, 2007) and intracranial recording studies (Brazdil et al., 2002; Wang, Ulbert, Schomer, Marinkovic, & Halgren, 2005), to critically rely on the dorsal anterior cingulate cortex (ACC) and surrounding medial prefrontal cortex (PFC; Bush, Luu, & Posner, 2000; Ridderinkhof, Nieuwenhuis, & Braver, 2007; Taylor, Stern, & Gehring, 2007). Although the exact neurocognitive process subserved by the dorsal ACC remains currently debated, its selective involvement in error detection and conflict monitoring is now well established.

According to the error-based reinforcement learning model (or alternatively, the risk prediction/error avoidance model, see Ridderinkhof, van den Wildenberg, Segalowitz, & Carter, 2004) the dorsal ACC receives feedback from the striatum and mesencephalic dopamine system (Holroyd & Coles, 2002; Brown & Braver, 2005), consistent with a functional link between cognitive monitoring and affective-motivational processes. In this model, errors are followed by a phasic suppression of dopamine, which increases the dorsal ACC activity, and in turn elicits the Error-Related Negativity (ERN), a well-known scalp ERP marker of error detection (see Falkenstein et al., 2000). Thus, the ERN is thought to reflect a cognitive signal that rapidly informs about a discrepancy between actual and expected outcome, and thus promotes learning (Holroyd & Coles, 2002; Frank et al., 2005).

There are also strong anatomical connections between rostral parts of ACC and other limbic structures involved in affect and motivation, such as the amygdala and insula (van Hoesen, Morecraft, & Vogt, 1993; Ongur & Price, 2000; see also Ochsner & Gross, 2005; Kienast et al., 2008). Based on this evidence, some theories proposed that ACC activity following errors could also reflect an appraisal of the affective significance or salience of errors (Luu, Tucker, Derryberry, Reed, & Poulsen, 2003; Hajcak, Moser, Yeung, & Simons, 2005; Pizzagalli, Peccoralo, Davidson, & Cohen, 2006; Taylor et al., 2006; Polli et al., 2008, 2009; Li et al., 2008; Hajcak & Foti, 2008). Consistent with this notion, the amplitude of the ERN is modulated not only by manipulations such as the frequency of errors (as predicted by the error-based reinforcement learning model, see Gehring, Goss, Coles, Meyer, & Donchin, 1993; Hajcak et al., 2003b), but also by motivational and emotional factors unrelated to the dopaminergic reward system, such as changes in state or trait anxiety (see Hajcak, McDonald, & Simons, 2003a, 2004; Vocat, Pourtois, & Vuilleumier, 2008; see also Pizzagalli et al., 2006). Further, in a recent scalp ERP study in healthy participants, Hajcak & Foti (2008) found that the startle blink reflex was enhanced following errors during a flanker task, suggesting that error monitoring could also activate the defensive motivational system responsible for the startle reflex (Lang, Bradley, & Cuthbert, 1990). Because both the

amygdala and insula are implicated in anxiety and defensive behaviors, these limbic regions might also contribute to error detection processes taking place in dorsal ACC (Ochsner & Gross, 2005; Fales et al., 2008; Kienast et al., 2008). Indirect evidence in support of this theory comes from a few neuroimaging studies that showed increased activity to errors not only in ACC and PFC, but also in deeper limbic brain structures such as the amygdala, insula, and thalamus (Menon, Adleman, White, Glover, & Reiss, 2001; Garavan, Ross, Murphy, Roche, & Stein, 2002; Polli et al., 2008; Li et al., 2008). In a recent fMRI study, Polli et al. (2009) reported an interesting association between the amygdala and rostral ACC during action monitoring, although reliable differences between the left and right amygdala were found in this study. Whereas activation in the right amygdala and right rostral anterior cingulate cortex predicted greater accuracy, the left amygdala activation predicted a higher error rate (see Polli et al., 2009). These results further emphasize that beyond the dorsal/rostral ACC, the amygdala is also involved in action monitoring, and they suggest different roles of the left vs. right amygdala in this process.

However, to date, few data exist to support a role for the human amygdala in error processing and, more generally, action monitoring. It still remains unknown whether mesio-temporal lobe structures, directly involved in emotional processing and learning (Phelps & LeDoux, 2005), might be recruited following errors (see Polli et al., 2008, 2009), and if so, at which latencies relative to the dorsal cingulate cortex. To our knowledge, only one single neurophysiological study reported intracranial ERPs to errors with recordings from mesio-temporal lobe structures, including the amygdala and hippocampus, in epileptic patients (Brazdil et al., 2002). Using a visual oddball task, these authors observed that medial temporal regions generated an ERN-like component (as well as a later positivity) to rare commission errors, with a similar latency (85-120 ms post response) than the scalp ERN (simultaneously recorded at CPZ electrode sites in these patients). The authors suggested that mesio-temporal lobe, in addition to ACC, may constitute an integral component of the brain's error checking system (Brazdil et al., 2002), but their electrophysiological data provided no specific distinction between error monitoring processes in these different regions.

Here, we could further examine this issue by having the unique opportunity to record iLFPs concurrently from the left amygdala, left hippocampus, and left dorsal anterior cingulate gyrus in a rare patient (SG), who was implanted with depth electrodes concurrently in these regions prior to surgery (Fig. 1). Our patient performed a speeded go/nogo task with non-emotional stimuli, previously validated in healthy participants and specifically designed to study error monitoring functions in clinical populations (Vocat et al., 2008). We predicted that error-related activity in the dorsal anterior cingulate gyrus should share some electrophysiological characteristics with the scalp ERN (such as an early latency relative to motor execution, as well as a dominant theta and beta spectral content; see Van Veen & Carter, 2002; Luu, Tucker, & Makeig, 2004; Debener et al., 2005), while a distinct pattern might arise in the amygdala, with early and/or later latencies (Hajcak & Foti, 2008). The unique combination of electrodes in patient SG allowed us to directly compare for the first time, in the same individual, the precise electrophysiological responses evoked by commission errors in these distant brain regions. Furthermore, to ensure that iLFPs recorded in these sites reflected local activity rather than electrical propagation from other nearby regions, SG also underwent an fMRI experiment during the same speeded go/nogo task, so

as to confirm a differential involvement of the dorsal cingulate cortex and amygdala in error processing. Finally, because patient SG had all depth electrodes implanted in the left hemisphere, we also recorded iLFPs from the right amygdala and hippocampus in a second patient (Fig. 1) during the same go/nogo task, allowing us to verify whether the pattern of activity found in the left amygdala of SG could be replicated for the opposite (right) amygdala, or was instead specific for the left hemisphere, contralateral to the hand used to make key-press responses.

Methods

Our two patients (SG and VM) were examined by invasive intracranial EEG monitoring with depth and subdural electrodes, in the context of presurgical investigations, following the usual clinical procedure at Geneva University Hospital (Seeck & Spinelli, 2004; Brodbeck, Lascano, Spinelli, Seeck, & Michel, 2009). At the time of testing, both patients were free of any medication, according to a standard weaning protocol during the intracranial recordings. No seizure was observed during or between our recordings. In addition, patient SG also participated to an fMRI session, after removal of the electrodes. Because of clinical schedule, VM could not undergo fMRI.

Case descriptions

Patient SG

SG is a 39-year-old right-handed man suffering from complex partial seizures in the left temporal lobe. Several neuropsychological and clinical neurological exams showed normal cognitive functions and normal intelligence. He had febrile convulsions as a child (10 months old), and presented with episodes of faintness and loss of consciousness when 20-years-old. In recent years, SG had many hyperkinetic seizures (up to 10 per month) which were characterized by an initial prickling of the upper right lip, interruption of current activities, language distortions (occasionally with swearwords), and finally complex motoric activities. During postictal periods, he complained about a marked tiredness. Several MRI scans confirmed a sclerosis of the left hippocampus, with hypoplasia of the splenium, and periventricular heterotopias. Clinical EEG recordings disclosed epileptic activity originating from the left frontal and medial temporal lobes. He was implanted with intracranial electrodes to better localize the initial epileptic focus, prior to surgical treatment. These electrodes targeted the left amygdala and left hippocampus (Fig. 1ABC), as well the periventricular heterotopias (Fig. 1A), but the latter electrodes also included a few sites placed in the depth of the left dorsal anterior cingulate gyrus (Talairach coordinates of the main contact in cingulate gyrus: -25x, -8y, +38z).

Patient VM

VM is a 54-year-old right-handed woman with left temporal lobe epilepsy since infancy (11 months). Several neuropsychological and clinical neurological exams showed asymmetries

in memory during interictal periods, with worse performance on verbal than visual memory tasks and mild language anomalies (paraphasia). A transient amnesia typically followed her seizures. The latter events (up to 4 per month) were characterized by an epigastric aura, followed by palpitations, loss of contact, bimanual automatisms, slow deviation of the head and eyes towards the left side, and eventually aphasic deficits and mutism. MRI scans revealed a sclerosis of the left hippocampus, with a relative diffuse atrophy of the left hemisphere. PET scans between seizures demonstrated a left mesio-temporal hypo-metabolism. However, EEG recordings during interictal periods showed epileptic spikes predominating over the right hemisphere; and recordings during seizures revealed a clear focus in the right hemisphere. Epileptic spikes (in the theta band) were also found to originate from the left temporal lobe (during interictal periods), with a slowing of background EEG rhythms during pre-ictal periods. VM was implanted with intracranial electrodes to better localize the epileptic focus prior to surgical treatment. Electrodes were placed in the left and right amygdala and hippocampus (Fig. 1DE), but for our study we focus on the right side (Fig. 1DE) because recordings from the left mesio-temporal electrodes were profoundly contaminated by frequent epileptic spikes (associated with the marked left hippocampus sclerosis in this patient).

Stimuli and task during intracranial recordings

We used a paradigm inducing a large number of errors in a short time, without excessive frustration, and validated by previous EEG work in normal healthy participants (Vocat et al., 2008). Visual stimuli consisted of an arrow presented centrally on a white background, oriented either upward or downward, but with different colors. Each trial started with a black arrow (upright or inverted), shown for a variable duration of 1000–2000 ms. This black arrow was then replaced by a color arrow (green or turquoise) at the same central location, with either the same or the opposite (180° inverted) orientation. This color arrow remained on the screen until the patient's response (on Go trials) or for a maximum of 1500ms (on Nogo trials). The inter-trial intervals (ITIs) included a blank screen of 500 ms, followed by a central fixation cross for another 500 ms. Participants were instructed to press the response key as fast as possible whenever the black arrow turned green and kept the same orientation (Go trials); but to withhold responses (nogo trials) if the black arrow turned green but changed orientation, or if it turned turquoise (irrespective of orientation). This manipulation provided two types of Nogo trials (based on orientation or color, respectively).

The experiment was divided into three sessions, each starting with a calibration block, immediately followed by two consecutive test blocks (60 trials each: 40 go, 10 orientation nogo, and 10 color nogo). Trial type was randomized within blocks. The whole experiment included 360 trials and lasted on average 20 min. During each calibration block, the mean RT for go trials was calculated online and used to define an upper response limit for correct go trials in the subsequent test blocks. Participants were never informed about this procedure, but during test blocks, they received a feedback about their speed of decision after each go trial. When a correct go response was made with RT above the upper limit, a deadline feedback screen was displayed with the French words "too late" in a red frame (shown for 500 ms); these correct trials were subsequently classified as "Slow Hits" and intended to maintain speed pressure (Vocat et al., 2008). No visual feedback was displayed

after correct responses made with RT below the upper limit (“Fast Hits”), or after the critical nogo errors (classified as “Color False Alarms” or “Orientation False Alarms” depending on whether the error was due to incorrect judgments of color or orientation, respectively). However, participants were informed that correct but slow responses were also considered as errors (see Fig. 2). As shown previously (Vocat et al., 2008), this procedure promoted the occurrence of many errors, due to irrepressible responses on nogo trials (commission errors).

To ensure a constant awareness of task performance in the participant, cumulated accuracy (in %) was continuously updated and displayed in the upper part of the screen during each inter-trial interval. The patient was also asked to report verbally his/her errors to the experimenter, after each response, whenever an error was thought to be made. These reports were recorded by the experimenter (by pressing a separate key), and served as an online measure of awareness of errors. Stimulus presentation and response recording were controlled using E-Prime software (V1.1, http://www.pstnet.com/products/e-prime/).

Stimuli and task during fMRI

During fMRI, patient SG performed a similar speeded go/nogo task as during the intracranial recordings session, although a few methodological changes were needed to make this go/nogo task compatible with the sluggish temporal resolution of fMRI and the rapid succession of events embedded within each of the trials. Unlike EEG, fMRI did not allow us to probe brain activity separately for the imperative stimulus, motor response, or the feedback, but measured a compound activity integrating these different events in a single condition.

There were two separate runs, each with 144 trials (96 go and 48 nogo) in random order (event-related design). Go and nogo trials were similar to those used in EEG recordings (see above). In addition, to establish a low-level baseline, each fMRI run also included 24 “control” trials (12 at the beginning and 12 at the end of each run). On these control trials, a red arrow (pointing either up or down, 12 per orientation) was presented for 1000 ms (constant ISI of 1000 ms), and the task required only a discrimination of its orientation (up vs. down) without any overt time pressure. The patient was instructed to use 2 buttons of a MRI-compatible response pad to decide whether the arrow presented was either pointing up or down. These control trials then allowed us to subtract out the main effect of sensory and motor components, and to determine activation selectively evoked by error monitoring processes during the go/nogo task.

A second adaptation during fMRI was to provide a feedback (positive or negative) after each trial for all task conditions, so as to avoid any systematic differences in the overall compound activity measured in different conditions. By contrast, during EEG, a visual feedback (“too slow”) was presented only after the “slow” hits (see above), but no feedback was given after errors and fast hits, to avoid any contamination of the intracranial ERP components around motor execution by concomitant visual inputs (and also to allow a direct assessment of error awareness). For go trials during fMRI (96/run), a positive feedback (green circle) was presented immediately after the key press when the patient was sufficiently “fast” on correct go trials (see below for exact timing procedure). But a negative

feedback (red circle) was presented when the patient was too “slow” on go trials. For nogo trials (48/run, 24 with color change and 24 with orientation change), the patient was shown the same “positive” feedback when he did not respond (correct rejections) or the same “negative” feedback when he made an incorrect key press (false alarms). Hence, the negative feedback did not discriminate between slow correct hits and false alarms.

Thirdly, during fMRI, the calibration of RTs (providing a flexible cutoff to distinguish between fast and slow hits, see Vocat et al., 2008) was made on a trial-by-trial basis, whereas we used the RT average over a whole block for this purpose during intracranial EEG (see here above). During fMRI, for any given go trial, the actual RT was always compared with the RT on the previous go trial. If the current RT was slower than the previous RT (i.e., using a strict criterion that the sum of current and previous RTs divided by two is lower than the current RT), the patient received a negative (red) feedback. If RT was faster than the previous one (i.e., the sum of current and previous RT divided by two is higher than the actual RT), the patient received a positive (green) feedback. This procedure ensured obtaining many false alarms despite fluctuations in speed on a trial-by-trial basis, because the arbitrary cutoff for correct responses was updated after each trial. We performed two training blocks before scanning to make sure that the patient understood correctly the task.

Finally, to yield a fixed time duration per trial (and hence a comparable duration of visual stimulation across experimental conditions) despite variations in RTs on individual trials, the inter-trial-interval was adapted online. This was achieved by continuously modifying the duration of the feedback as a function of RT (slow RTs were followed by shorter feedback durations and fast RTs by longer feedback durations; ranging between 500 and 1320 ms). This procedure ensured that the total duration of visual stimulation was similar (mean ~4000 ms) across the four critical conditions (fast hits, slow hits, commission errors and correct rejections), and that trials in each experimental conditions had a comparable sequence of events.

Intracranial recordings and data analyses

iLFPs were continuously recorded (Ceegraph XL, Biologic System Corps.) with a sampling rate of 512 Hz (bandpass 0.1–200 Hz) using depth electrodes (AD-Tech, electrode diameter: 6 mm, inter-electrode spacing: 10 mm, see Fig. 1). The reference electrode was located at position Cz and the ground at position FCZ in the 10–20 international EEG system. Intracranial evoked potentials were obtained by averaging LFPs time-locked either to stimulus or response onset, for each category separately (fast hits, slow hits, commission errors and correct rejections). Individual epochs were low-pass filtered using a 30Hz cutoff.

Electrode positions were determined by a brain CT-scan performed after implantation, and coregistered using SPM5 (http://www.fil.ion.ucl.ac.uk/spm/) to the patient’s brain anatomy as obtained with MRI, which in turn was normalized in order to define Talairach coordinates of each of the recorded electrodes.

Single-trial EEG epochs (-500/+1500ms around either the stimulus or response onset) were analyzed offline, after removing all epochs where noise or possible epileptic spikes might have spread and contaminated the recorded sites (~10% on average in patient

SG and ~20% on average in patient VM, using stringent selection). The amplitude variance computed for each time-point across spike-free trials was then used as dependent variable for statistical comparisons. To verify that event-related intracranial responses were stable over time and across trials, we also computed an amplitude×time image (Delorme & Makeig, 2004) for all consecutive trials within an given experimental condition or according to RTs (see Fig. 4 for example).

The presence of significant differences between experimental conditions was determined by nonparametric statistical analyses based on stringent randomization tests (see Manly, 1991; Pourtois, Peelen, Spinelli, Seeck, & Vuilleumier, 2007 for similar approach). Randomization provides a robust non-parametric statistical method without any assumption regarding data distribution, by comparing the observed dataset with random shuffling of the same values over many iterations (i.e. permutations). Shuffling is repeated many times (minimum of 5000 with the randomization tests used here) so as to estimate the probability (here $p < 0.01$) that the data might be observed by chance. The significant alpha cutoff was set to $p < 0.01$, with an additional criterion of temporal stability for at least 5 consecutive time-points (10ms at 512 Hz sampling rate). Importantly, because errors were less frequent than either fast or slow hits, we always run the statistical analyses by using a similar number of trials per condition. This was achieved by randomly selecting a subset of (fast or slow) hits, in such a way to obtain the same number of fast or slow hits, compared to errors. These statistical analyses were performed using Cartool software developed by Denis Brunet (http://brainmapping.unige.ch/Cartool.php).

To evaluate systematic changes in the spectral content of intracranial data recorded in the left dorsal cingulate gyrus and left amygdala, we performed several auxiliary time/frequency decompositions (Fig. 7) using the short-time Fourier transform, a sinusoidal wavelet transform, implemented in the EEGLAB toolbox (Delorme & Makeig, 2004). Perturbations in the spectral content of the data were estimated by windowed sinusoidal functions (mathematical details are given in Delorme & Makeig, 2004). Using this method, we could reveal transient event−related spectral perturbations (ERSPs), which corresponded in this case, to event−related shifts in the power spectrum (see Makeig, 1993). Finally, we also determined the degree of synchronization between the left dorsal cingulate cortex and left amygdala (Fig. 7GHI), using a measure of event−related cross−coherence between these two distant regions (Rappelsberger, Pfurtscheller, & Filz, 1994; Essl & Rappelsberger, 1998; Delorme & Makeig, 2004). Synchronization was determined by using a measure of coherence magnitude (expressed as an index varying between 0 and 1, where 1 represents two perfectly synchronized signals).

fMRI data acquisition and analyses

MRI data were acquired using a 3T Trio system (Siemens) with parallel imaging (GRAPPA) from an 8-channel headcoil. Structural images were acquired with a T1-weighted 3D MPRAGE sequence (176 contiguous sagittal slices, FOV=256*240mm, TR/TE/TI/Flip angle = 2500ms/2.8ms/1100ms/8°, matrix=256*240, slice-thickness=1mm) and functional images with a gradient-echo EPI sequence (TR/TE/Flip angle = 1100ms/27ms/90°, FOV=240mm, matrix=64x64). Each functional image comprised 21 axial slices (voxel size: 3.75x3.75mm;

thickness 4.2mm; gap 1.05mm) oriented parallel to the inferior edge of the occipital and temporal lobes. A total of 1259 functional images were acquired across two runs, separated by a brief pause.

Functional images were analyzed using SPM2 (www.fil.ion.ucl.ac.uk/spm/). All images were realigned, corrected for slice timing, spatially smoothed (10 mm FWHM Gaussian kernel), and high-pass filtered (cutoff 128s). Individual events were modeled by a standard synthetic haemodynamic response function (HRF). Five conditions (event types) were defined: control trials (in blocks where the task required discriminating the orientation of red arrows without time pressure), as well as fast hits, slow hits, nogo correct (correct inhibition) and errors (false alarms). Movement parameters from spatial realignment (3 translations, 3 rotations) were also entered as covariates of no interest in statistical analyses to account for residual movement artifacts. The general linear model (Friston et al., 1998) was then used to generate parameter estimates of activity at each voxel, for each condition. Statistical parametric maps were generated from linear contrasts between parameter estimates from the different conditions. We report regions that survived $P < 0.001$ uncorrected, with a cluster size of more than 5 contiguous voxels. Contrast images were normalized to the Talairach template, providing peak coordinates for activations in the amygdala and ACC that could be directly compared with the estimated location of intracranial electrodes.

Results

Behavioral and brain data were analyzed separately for the 4 critical trial types: errors (i.e. false alarms on nogo trials), “fast” hits (i.e. correct responses on go trials, with RTs below the cutoff value based on calibration blocks), “slow” hits (i.e. correct responses on go trials but slower than RT cutoff, therefore followed by a visual feedback indicating “too slow”), and correct rejections (i.e. successful inhibition of response on nogo trials). However, the critical comparison concerned errors vs. fast hits, which constituted opposite outcomes but were produced with similar RTs (see Fig. 2). Hence, this comparison was not confounded by any substantial RT difference (potentially arising from differences in motor preparation and/or motor execution). No analyses were run separately for the two error types, orientation FA vs. color FA, mainly because of the small number of trials for each condition.

Behavioral results

Consistent with behavioral results in normals (Vocat et al., 2008), the two patients made a substantial number of false alarms (commission errors) on nogo trials, while they made no omissions on go trials (Fig. 2A)

During the intracranial recording session, patient SG was 100% correct on go, but 68% correct on nogo trials. VM was also at ceiling with go (100% correct) but correctly withheld responses on 68% of nogo. Among correct go trials, 67% were slow hits (vs. 33% fast hits) in SG, whereas 44% were slow hits (56% fast hits) in VM. For the two patients, the error rate fell within the range (95% confidence interval) obtained in a group of 16 healthy

adult participants (Vocat et al., 2008). All errors made on nogo trials were verbally reported by both patients (see methods), suggesting preserved error monitoring and awareness.

During the fMRI session, patient SG was again 100% correct on go trials (54% slow, 46% fast hits), but made slightly more false alarms on nogo trials (40% correct) compared to the intracranial EEG session (Fig. 2A). This difference was likely to result from the more severe cutoff used to distinguish between fast and slow hits during fMRI (in keeping with overall faster RTs relative to the intracranial EEG session).

Analyses of median RTs confirmed that patients responded rapidly to the imperative stimulus (go trials), and importantly, showed similar RTs for fast hits and commission errors (patient SG: 275 vs. 292 ms; patient VM: 344 vs. 318 ms), as intended by our speed pressure procedure (Fig. 2B).

Finally, each patient showed a systematic RT adjustment following errors (Fig. 2B; see Rabbitt, 1966; Laming, 1968), indicated by slower RTs on go trials following an error, as compared with go trials preceded by another correct go trial (Mean ± 1 S.E.M.; SG: 348 ± 10 ms vs. 333.5 ± 5 ms; VM: 474.5 ± 31 ms vs. 426 ± 10 ms). The same effect was seen during the fMRI session in patient SG (279.5 ± 8 ms vs. 268.3 ± 4 ms). However, we found no differential neural effect in amygdala or ACC related to the post-error slowing effect, and do not report EEG or fMRI results separately for these conditions.

Intracranial results

For both the anterior cingulate and amygdala electrodes, we first report results for stimulus-locked ERPs, and next those for response-locked ERPs (Fig. 3). Stimulus-locked vs. response-locked ERPs were computed separately to determine to which extent the amygdala and the dorsal cingulate gyrus showed perceptual vs. decisional effects during the go/nogo task. Analyses of Stimulus-locked ERPs were also important to explore electrophysiological changes in the correct rejection condition, where no overt response (but only a nogo visual stimulus) was recorded. As it turned out, both the left dorsal cingulate gyrus and amygdala showed strong ERP modulations around the response, consistent with their involvement in action monitoring.

Left dorsal anterior cingulate (Patient SG)

Stimulus-locked ERPs from the left anterior cingulate gyrus revealed that this region reacted to lapses of cognitive control (Fig. 3A). A biphasic, mainly positive activity started ~100 ms after onset of the imperative stimulus, followed by a more sustained negative activity after a peak at ~250 ms. Because SG had a mean RT of 307 ms (across the different conditions), it is likely that these components were not exclusively related to sensory processing of the imperative stimulus, but instead reflected a post-perceptual stage (as confirmed by response-locked ERPs, see below). Whereas all four conditions generated a similar initial positive activity, commission errors generated an extra positivity ~250 ms post-onset, which in turn altered the subsequent negative component (Fig. 3A). In other words, all correct conditions were similar (despite the different response outcomes such as hits and correct

rejections) but they selectively differed from errors (false alarms). These amplitude differences could not be easily explained in terms of conflict monitoring (here presumably triggered by the stimulus), as it turned out that correct rejections clustered together with fast and slow hits (see Fig. 3A), whereas errors clearly elicited distinctive brain responses in this dorsal ACC region. Presumably, the amount of stimulus-locked conflict was the same between nogo trials that eventually led to errors, and nogo trials that eventually led to correct rejections. Nonetheless, stimulus-locked ERPs in the dorsal ACC were similar for these two conditions (Fig. 3A), whereas response-locked ERPs were quite different (Fig. 3B).

These observations were confirmed by statistical comparisons (using pairwise permutation tests on all single trials, see methods). First, comparing iLFPs for errors vs. fast hits (two conditions with similar RTs) showed a reliable difference ($p<0.01$) starting 246 ms and lasting up to 596 ms following stimulus onset (Fig. 3A). In other words, the cingulate generated a reliable accuracy signal ~40 ms before the patient had actually hit the key (median RTs on nogo errors: 291 ms). Second, comparing iLFPs for commission errors vs. correct rejections (two conditions with the same nogo stimulus but different responses) revealed a reliable difference ($p<.01$), from 322 ms up to 689 ms following onset. Finally, a comparison of fast hits vs. correct rejections (in which both the imperative stimulus and motor response were different, but the outcome was correct) disclosed a significant difference ($p<.01$) from 264 to 316 ms following onset, with a broader early positive activity for correct rejections than fast hits. However, importantly, the subsequent negative component was not statistically different between these two conditions (Fig. 3A). Combined together, these statistical comparisons pointed to a selective involvement of the dorsal anterior cingulate in error detection starting ~250 ms after stimulus onset, during a time period where the participant was still preparing (but not yet executing) his motor response, whereas there was no clear effect of the actual motor response (i.e. key-press on fast hits, but not on correct nogo trials).

Similar analyses made on the response-locked ERPs from cingulate gyrus confirmed this pattern. A first positive ERP component starting before RT was followed by a broad and sustained negative component. Errors started to differ from fast hits just before RTs, when the positive component reached its maximum amplitude (peak latency: 66 ms before RT; peak amplitude: 33.8 μV), with an extra positive activity (peak latency: 31 ms after RT, amplitude: 31.4 μV) that profoundly altered the expression of the subsequent negativity (Fig. 3B and Fig. 4ABC). The latter component was markedly delayed for errors relative to fast hits (285 ms vs. 150 ms post RT). In contrast, fast and slow hits showed only a latency difference: the positive activity started and peaked earlier for slow hits (113 ms before RT) than either fast hits (70 ms before RT) or errors (66 ms before RT) (Fig. 3B). These observations were confirmed by statistical analyses. Pairwise comparison between errors and fast hits revealed a significant divergence ($p<.01$) from 49 ms to 264 ms following RT, confirming a detection of errors in this cingulate region prior to the actual key-press. But there was no amplitude difference between slow and fast hits. A trial-by-trial breakdown (Delorme & Makeig, 2004) for each condition separately (Fig. 4ABC) confirmed that these two ERP responses were consistent over time, with no systematic learning or habituation effect.

Finally, for each condition separately (errors, fast hits, and slow hits), we run a statistical analysis to determine the onset (and duration) of the early positive activity

preceding RTs. We used the first 250 ms of individual epochs as a reference baseline, and then calculated when (and how long) the ERP waveform differed relative to this baseline. For errors, the early positivity spanned from 127 ms before RTs to 125 ms after RTs (Fig. 3B; $p<.01$). For fast hits, it spanned from 131 ms to 25 ms before RTs ($p<.01$). By contrast, for slow hits, this positivity was earlier and broader, from 227 ms to 35 ms before RTs ($p<.01$). These results suggest an inverse relationship between the early positivity and RTs, namely, the earlier the positivity, the longer the RTs. This assumption was further verified by a direct correlational analysis of individual trials (ERP image Delorme & Makeig, 2004), in which the early positive activity was sorted according to response speed. As illustrated in Fig. 6AB, the slow hits (but not errors and fast hits) showed a highly significant correlation (Pearsons $r=.49$, $p<.001$) between the positive peak and actual RT across trials ($n=147$), indicating that slower RTs were associated with an earlier positive peak (relative to RT onset). These results suggest a functional coupling between behavioral speed and this positive activity, likely reflecting motor preparation (or execution) taking place in the cingulate motor area (Ullsperger & von Cramon, 2003). Although the early positive activity preceding RTs was inversely related to speed for slow hits (see Fig. 6A), we did not find any modulation of the neural activity following RTs as a function of speed, in none of the three conditions (slow hits, fast hits and errors). However, in a previous scalp-ERP study, the authors found larger error-related brain activity (ERN) for “late” (but still correct) responses, relative to fast (and correct) responses (see Luu et al., 2000). There are a number of methodological differences between the present experiment (using a Go–noGo task leading to a low variability in RTs, see also Fig. 6) and the study of Luu et al. (2000, using a flanker task leading to a higher variability in RTs), which could potentially account for the fact that we did not observe in our study any reliable difference for the amplitude (or latency) of neural activities following motor responses between fast and slower (correct) hits within the dorsal ACC.

Altogether these results suggest that ACC precisely kept track of response accuracy, and that an error signal was generated in this region ~50 ms before RTs (Fig. 3B). While two distinct ERP components were measured in this region, an initial positivity just prior to RTs, was likely to reflect motor preparation, as its amplitude was inversely related to response speed (Fig. 6), and a subsequent larger negativity was specifically sensitive to false alarms, presumably reflecting error monitoring per se (Fig. 4ABC).

Left amygdala (Patient SG)

While the dorsal cingulate region showed a “quasi immediate“ response to errors, a very different pattern was recorded from the left amygdala in the same trials, for the same patient (Fig. 3CD).

Unlike the cingulate, the amygdala exhibited a significant ERP only to conditions with an actual key-press (i.e., go trials and false alarms, but not correct rejections, see Fig. 3C), which was characterized by an ample monophasic positive activity. Stimulus-locked ERP analyses (Fig. 3C) indicated that this activity occurred close to motor responses. More importantly, response-locked ERPs (Fig. 3D) revealed systematic latency differences for this positivity between the three response conditions (errors, fast hits, and slow hits). The positive component had an early peak around RTs, with a slight delay for fast hits (latency: 96 ms

post RT; amplitude 85.1 μV) relative to slow hits (25 ms; 80.8 μV), but a much longer latency for errors (320 ms; 83.4 μV). This substantial latency shift is striking, given that the median RT for errors (291.5 ms) was only ~15 ms longer than fast hits (275 ms), whereas slow hits (median RT: 370.5) were ~100 ms longer than fast hits, suggesting that these ERPs did not merely reflect differences in speed across conditions (see Fig. 2 and Fig. 3C). Hence, there was no relationship between the latency (and/or amplitude) of this positive activity and the speed of motor responses (RTs; see Fig. 6C).

Statistical analyses of response-locked ERP data corroborated these observations. Relative to a 250 ms baseline period, a significant positive ERP deflection arose from 70 ms before RTs up to 225 ms after RTs for slow hits; from 39 ms before RTs up to 279 after RTs for fast hits; but started 158 ms *following* RTs and lasted up to 473 ms for errors (all $p<.01$ compared to baseline). In addition, in the slow hits condition, the presentation of a visual feedback after response evoked a small but distinct negative deflection ~700 ms after RTs, which was not seen for fast hits where no visual feedback was presented. Direct pairwise statistical comparisons (permutations) confirmed significant ($p<.01$) latency differences for this positive deflection in the left amygdala between the three experimental conditions (slow hits, fast hits, and errors). The positivity was earlier ($p<.01$) for slow hits than either fast hits or errors (Fig. 3D), and earlier ($p<.01$) for fast hits than errors (Fig. 3D).

Moreover, a direct comparison between the left amygdala and left cingulate showed systematically earlier effects in the latter than the former region (i.e., slow hits: 70 ms vs. 227 ms before RTs; fast hits: 39 ms vs. 131 ms before RTs; errors: 158 ms after RTs vs. 127 ms before RTs; for amygdala and ACC respectively), suggesting that errors were first detected in the dorsal cingulate before modulating the amygdala at a later stage of processing. Thus, for errors, an average ~280 ms elapsed between the first positivity in the cingulate and the first positivity in the amygdala, whereas ~90 ms elapsed between responses in these two regions for fast hits (despite similar RTs). However, even in the amygdala, the positive deflection recorded on fast and slow hits already started a few tens of ms before RTs, suggesting a rapid involvement of the amygdala in action monitoring, while it was selectively delayed on commission errors (Fig. 4DEF).

A trial-by-trial breakdown (Delorme & Makeig, 2004) for each condition separately (Fig. 4DEF) also confirmed that this positivity in left amygdala was consistent over time, for both latencies and amplitudes, with no systematic learning or habituation effect. Furthermore, in contrast with the cingulate gyrus, there was no relation to motor speed when sorting individual trials as a function of RTs (Fig. 6C), further suggesting a different functional role during action monitoring.

Finally, we performed a series of additional analyses to verify whether these responses recorded at amygdala electrode sites were most likely generated in this region, or alternatively, spreading from other nearby regions in mesio-temporal lobe (such as the adjacent anterior hippocampus), or even deeper brain structures (see Brazdil et al., 2002; Holroyd & Coles, 2002). In support of a direct amygdala origin, we found an amplitude gradient for the recorded positivity from the more medial electrode (maximum amplitude, centered in amygdala) to the more lateral electrode (located in peri-amygdala regions, see Fig. 5CDE). Moreover, the comparison of iLFPs from the left amygdala and left hippocampus demonstrated a striking polarity reversal (Niedermeyer & Lopes da Silva, 2004), with an

ample positivity in the former but an symmetrical negativity with a similar latency in the latter region (Fig. 5ABC). This polarity reversal provides a distinctive neurophysiological marker pointing to a local neural generator situated between the two electrodes (Creutzfeldt & Houchin, 1974). Here, although the negative peak was slightly delayed (by ~70 ms) in the hippocampus relative to the amygdala for slow hits (105ms vs. 25ms) and fast hits (164ms vs. 96ms), this was reversed for errors (262ms vs. 320ms), again emphasizing the distinctiveness of error events for the left amygdala.

Oscillations (Patient SG)

The spectral content of iLFPs recorded from the left dorsal anterior cingulate and left amygdala were also found to be qualitatively different (Fig. 7). The left amygdala showed a transient and selective increase in the theta band (~ 5 Hz) coinciding with motor execution (Fig. 7 DEF), with no other systematic event-related perturbations in other frequency bands. Consistent with the ERP results above, this transient increase occurred slightly earlier for slow hits (Fig. 7D), than fast hits (Fig. 7E), but was markedly delayed for errors (Fig. 7F). Furthermore, for errors only, this transient increase in theta power was expressed by two successive bursts (Fig. 7E), rather than a single burst as in the other two conditions. By contrast, the cingulate exhibited a large and sustained decrease in the alpha band (~ 10 Hz) starting at the time of motor execution (Fig. 7ABC), preceded by a smaller increase in theta just prior to the RTs. The decrease in alpha power was followed by a rebound increase in beta power (22-26 Hz) ~ 500 ms after motor execution (most likely corresponding to a post-movement beta rebound, see Parkes et al., 2006), but only for the slow (Fig. 7A) and fast hits (Fig. 7B), not for errors.

Remarkably, coherence analyses revealed that these two brain regions also became transiently synchronized, selectively in the low theta (and delta) band (i.e., $\leq$ 4 Hz), and across all conditions (Fig. 7GHI). This synchrony arose mostly during the same time period as the theta increases in amygdala (slow hits: from -100 to +50 ms; fast hits: from -50 to +100 ms; errors: from +100 to +250 ms relative to motor execution).

Right amygdala (Patient VM)

This second patient was implanted with depth electrodes in the right amygdala and hippocampus (Fig. 1DE), offering the unique opportunity to verify and extend our previous findings concerning a role for the amygdala in action monitoring, but in a different patient and a different hemisphere. However, patient VM was not implanted in cingulate regions (unlike SG who underwent a combined implantation due to his unusual heterotopias in deep brain structures).

Although electrophysiological data were slightly noisier in VM than SG, a similar positive ERP component was recorded around motor executions (RTs) in her right amygdala (Fig. 8), with the exact same shift in latency for errors relative to fast hits (even though the mean RT difference between errors and fast hits was < 30 ms in this patient). Response-locked ERPs revealed that the component peaked 53 ms after RTs for fast hits (amplitude: 29.3μV), but 311 ms after RTs for errors (amplitude: 35.1μV), resulting in ~260 ms delay

between these two conditions, similar to our findings for the left amygdala in patient SG. A direct statistical comparison between conditions confirmed that fast hits elicited a larger ($p<.01$) positive component during an early time period from 8 to 98 ms after RTs, whereas errors elicited a larger positive component during a later time period from 268 to 396 ms after RTs (Fig. 8A). Relative to the initial 250 ms baseline of individual epochs, the fast hits were found to produce a positive deflection differing from baseline ($p<.01$) from 80 ms before RTs up to 160 ms after RTs; whereas errors produced a significant deflection ($p<.01$) starting only 246 ms after RTs and lasting up to 502 ms after RTs (Fig. 8A).

A trial-by-trial breakdown (Delorme & Makeig, 2004) for each condition separately (Fig. 8CDE) also confirmed that this response was reliable at the single trial level, with no systematic change over time.

We note that, unlike fast hits and errors, slow hits did not elicit a comparable positive component around or after RTs in the right amygdala of this patient (Fig. 8A), in contrast to the left amygdala of patient SG for the same condition. One possible explanation might stem from the fact that patient VM showed a much more pronounced RT difference (~ 210 ms) between fast hits and slow hits than patient SG (~100 ms), such that, slow hits were not very different from fast hits for SG but more distinguishable in VM (see Fig. 2). This could leave some "extra" processing time for VM to assess accuracy of her behavior, perhaps with a less rapid and systematic involvement of appraisal mechanisms in the amygdala (Fig. 8A), in contrast to responses made in a more impulsive or uncertain way (i.e. fast hits and errors, Fig. 8A).

Another striking electrophysiological similarity between the two patients concerned a conspicuous polarity reversal for this intracranial positivity (Fig. 8B), again found between the amygdala (positive peak) and the adjacent anterior hippocampus (negative peak), thus suggesting a local neural generator (Fig. 8B; compare with data for patient SG in Fig. 5A). Similarly to our findings for the left amygdala and hippocampus in patient SG, the polarity reversal between right amygdala and right hippocampus in patient VM also revealed a slight delay for the negative peak in hippocampus, relative to the positive peak in amygdala (Fig. 8B), for both fast hits (amygdala: 53ms/29.2μV; hippocampus: 145ms/-96.3μV) and errors (amygdala: 307ms/35.2μV; hippocampus: 438ms/-119.0μV)

Finally, time/frequency analyses (Delorme & Makeig, 2004) confirmed that the positive ERP response recorded in the right amygdala of patient VM around motor execution was mainly driven by selective event-related spectral perturbations in the theta band, similarly to what was observed for the left amygdala of patient SG (see above and Fig. 7).

fMRI results (Patient SG)

The differential contributions of the dorsal cingulate gyrus and amygdala to action monitoring were further established by using fMRI and the same go/nogo task in patient SG (patient VM was not available for fMRI). Our main goal was to verify whether activity recorded at amygdala electrodes during intracranial recordings was generated in the amygdala itself, rather than another nearby region close to these electrodes, and to determine how the

different time-course of electrical activity modulated the pattern of fMRI responses across task conditions.

In the scanner, patient SG performed a variant of the same go/nogo task, in which he made 58 false alarms (34 orientation FAs and 24 color FAs) out of 96 nogo trials, but no omissions on go trials (Fig. 2). His mean RT was 249 ms for errors, and 236 ms for fast hits, again allowing us to contrast these two conditions with opposite accuracy but negligible RT difference.

The critical comparison between errors and hits revealed a reliable ($p<.001$) bilateral activation in the dorsal cingulate cortex (Fig. 9AB). Parameter estimates of activity (betas) extracted for the peak activation on each side (left: -11x, -24y, +38z; right: +11x, -30y, +35z) confirmed that this region mainly responded to errors, as opposed to hits or correct rejections (Fig. 9B). A comparison with the Talairach coordinates of intracranial electrodes placed in the left cingulate gyrus (-25x, -8y, +38z) indicated that the peak of fMRI activation was located in a just slightly more posterior position (~15 mm) as compared with the cingulate electrode. These fMRI data therefore converge both functionally and anatomically with the intracranial results obtained from the cingulate in the same patient.

A significant ($p<.001$) bilateral activation of the amygdala was also found (Fig. 9C), primarily revealed by contrasting fast hits to errors. As can be seen in Fig. 9, the response profile of the amygdala was different from that of the dorsal cingulate cortex, confirming their differential role during action monitoring. Parameter estimates extracted from the amygdala peak on each side (Fig. 9D; left: -20x, -2y, -21z; right: +17x, -9y, -27z) showed greater activation to all “correct” responses (including fast hits and correct rejections) as opposed to “incorrect” responses (including errors and slow hits), a pattern suggesting a sensitivity to the motivational or emotional relevance of the outcome of each trial. However, among correct trials, amygdala responses were slightly larger for successful motor action (fast hits) as compared with successful inhibition (correct rejections), which may further suggest an influence of the actual motor execution on amygdala activation.

Taken together, these fMRI results do not only confirm that the amygdala is involved in action monitoring, but also that its contribution is qualitatively different from the dorsal cingulate cortex (see Fig. 9).

Discussion

Whereas the functional mapping of the dorsal ACC and its involvement in errors detection has been greatly refined over the last decade by using fMRI and scalp EEG (see Debener et al., 2005; van Veen & Carter, 2006), the contribution of other brain structures, in particular the amygdala, to “cognitive” mechanisms of error monitoring has received much less attention and inconsistent support. However, in most cases, errors are not experienced as neutral events (Rabbitt, 1966; Hajcak & Foti, 2008). Errors are typically considered as rare, negative and interfering events, which need to be avoided, and can even activate the defensive/aversive motivational system (Hajcak & Foti, 2008). Accordingly, it is plausible that errors do not only influence cognitive mechanisms such as learning, attention, and memory, but also modulate affective states in order to promote adaptive and flexible behaviors

(Hajcak et al., 2005; Li et al., 2008). Nevertheless, very few studies have corroborated this assumption so far (see Brazdil et al., 2002), and the impact of errors on brain systems implicated in emotional appraisal remains largely unknown. Some preliminary evidence comes from functional neuroimaging studies that reported activations to errors in regions usually associated with emotional processing such as the amygdala or insula (Menon et al., 2001; Garavan et al., 2002; Polli et al., 2008, 2009; Li et al., 2008). However, these studies do not inform about the exact time-course of error processing, in particular in relation to successive stages of motor preparation, execution, and/or feedback signals. Likewise, although several scalp ERP studies reported a modulation of the ERN amplitude by emotional or motivational factors (Hajcak et al., 2003a, 2004; Holroyd & Coles, 2002; Hajcak et al., 2005; Pizzagalli et al., 2006; Vocat et al., 2008; Hajcak & Foti, 2008), none could relate these effects to the activation of deep brain structures involved in emotional processing, such as the amygdala or insula.

In our study, we had the unique opportunity to record intracranial ERPs from dorsal ACC and amygdala simultaneously, allowing us to demonstrate that the human amygdala participates to error detection, and to dissociate its responses from those of ACC. In contrast, Brazdil et al. (2002) primarily found similar error-related brain responses (i.e. ERN and Pe components) in distant and non-overlapping brain regions, including the amygdala, hippocampus and dorsal cingulate cortex. There are a number of important methodological differences (including the patients and their medical history, the stimuli, task, as well as intracranial electrodes, recording parameters and data processing) between our study and the pioneer study of Brazdil et al. (2002), which may somehow explain the discrepancy between these two studies, and which preclude any direct comparison between these two studies. Brazdil et al. (2002) used a simple (non-speeded) go/nogo task and their patients made very few errors (mean of 9 false alarms). By contrast, we used a speeded go/nogo task and the patients made a higher number of false alarms (~30-40 false alarms) within a shorter time. Hence, in the study of Brazdil et al. (2002), errors were clearly deviant, whereas in our study, they were more frequent, and the border with correct responses (i.e. fast hits) was made less clear. Accordingly, errors were likely to have a different impact on cognitive control systems in the study of Brazdil et al. (2002), compared to false alarms recorded in our study. Importantly, when errors were rare and they mostly corresponded to lapses of control or attention, the amygdala and dorsal cingulate cortex showed comparable early monitoring effects (see Brazdil et al., 2002). By comparison, these two regions showed distinct action monitoring effects when errors became more frequent and were less avoidable, to some extent (see also Vocat et al., 2008). Interestingly, these two situations could therefore lead to different action monitoring effects in the amygdala and dorsal cingulate cortex. Future intracranial ERP or fMRI studies should more directly address this question and assess under which conditions (including variations of task demands) these two regions (amygdala and dorsal ACC) may show similar or distinct action monitoring effects (see also Polli et al., 2009).

Our new results confirm that the dorsal anterior cingulate cortex is involved in performance monitoring (see Ridderinkhof et al., 2007 for a recent overview), but in addition show for the first time that the amygdala also generates an early differential signal for correct responses (hits) and errors (false alarms). This effect was essentially characterized by a striking delay of neural activity following errors. Thus, the amygdala responded ~150 ms after

incorrect key-presses but already ~40 ms prior to correct key-presses, while ACC activity started ~130 ms before motor responses in both cases but lasted 150 ms longer after errors than after correct key-presses. These findings suggest that error detection mechanisms did not only recruit brain systems typically involved in action monitoring and cognitive control, such as ACC (Ridderinkhof, Ullsperger, Crone, & Nieuwenhuis, 2004), but also activate limbic brain regions such as the amygdala, which is known to play a key role in affective processing and emotional learning (Phelps & LeDoux, 2005). Importantly, the same pattern of amygdala activity was replicated in two different patients, and for different hemispheres (left in SG, right in VM). In addition, our results show that these neurophysiological signals were generated at early latencies and during overlapping time-periods (around the time of motor execution) in both the amygdala and cingulate. Furthermore, these effects involved a transient coupling in the theta band between these two regions, with a slightly different time-course across the different task conditions. The early latency of these responses, in both ACC and amygdala, rules out a simple explanation based on the conscious appraisal of the actual (correct or incorrect) motor outcome, since this would predict that cognitive effects in ACC or emotional effects in amygdala should arise only at much later latencies after RTs. The transient increases in the theta band power demonstrated by our spectral analysis converge with previous results suggesting that error detection is tightly linked to brain rhythms in the theta band (Luu et al., 2004; Debener et al., 2005). Thus, our results also suggest that changes in the theta power spectrum that are characteristic of action monitoring (see Luu et al., 2004) might not necessarily reflect activity from the dorsal ACC in isolation, but instead, of a selective coupling between this region and a deeper brain structure, such as the amygdala.

Amygdala and behavioral relevance

A striking result in both patients was that the amygdala responses to correct key-presses (fast hits) and incorrect key-presses (false alarms) were markedly shifted in time by ~250 ms, although these two conditions were associated with similar RTs, allowing a comparison of errors and hits unconfounded by differences in motor speed (see Vocat et al., 2008). Therefore, this selective delay of amygdala responses to errors could not be explained by unbalanced RTs between experimental conditions. Moreover, these effects were consistently observed at the single trial level, without any apparent changes as a function of time elapsed during the experiment or as a function of motor speed (RTs). No such response was generated in the amygdala after correct rejections, that is, when the patients successfully inhibited a motor response on nogo trials. This suggests that a recruitment of the amygdala in action monitoring depended on the actual production of a motor response, being either correct or incorrect. Besides response accuracy, another factor influencing action monitoring in the amygdala might concern the level of uncertainty about one's own motor actions, which is presumably high when responses are fast and impulsive as in the present task (Vocat et al., 2008). Consistent with this view, amygdala responses were absent for correct rejections, and slightly delayed for fast hits as compared with slow hits in patient SG, possibly reflecting a lower uncertainty about performance in the latter case.

However, our simultaneous recordings from both sites in patient SG revealed that ACC activity always preceded amygdala activity (even prior to an executed motor action),

and that the response of the amygdala appeared to start at about the time when cingulate activity terminated. Interestingly, the theta coupling between the two regions was consistent with this precise temporal hierarchy. In keeping with the fact that cingulate responses to errors were prolonged by ~150 ms after motor execution, relative to correct fast hits, amygdala responses arose with a substantial delay after motor execution on error trials, unlike its early response around RT on correct trials. Thus, amygdala activity somehow appeared to index the closure of the action monitoring period taking place in ACC. When no mismatch between intended and executed action was detected, activity in ACC could terminate and then possibly trigger subsequent amygdala responses, whereas the processing of conflict signals between intention and execution could prolong ACC activity and therefore also delay amygdala responses. Moreover, because no reliable amygdala activity was observed when no action was produced, these findings suggest that the amygdala might integrate both motor signals and monitoring information, presumably in order to register the motivational significance of the action outcome based on the current behavioral goals.

In patient SG, fMRI results confirmed that activity recorded in the left amygdala by depth electrodes was produced locally, rather than picked up from another nearby neural generator. Bilateral amygdala activation could clearly be demonstrated in SG during the same go/nogo task. No significant activation was observed for errors relative to correct trials in adjacent regions within the temporal lobe or deeper brain structures. Remarkably, however, fMRI results indicated that bilateral amygdala evoked the largest BOLD response to fast hits, and to a lesser extent to correct rejections on nogo, as compared with smaller responses to errors or slow hits. These results are consistent with a role for this region in encoding the motivational relevance of motor actions, as it discriminated between correct and incorrect key-presses. However, this pattern of activation contrasts with the intracranial ERPs results showing a similar amplitude of iLFPs for errors and fast hits, but with delayed latencies. These findings might be consistent with a role for both motor and monitoring inputs in driving amygdala activation, with no significant BOLD response being evoked when signals are received from ACC with a delay after motor execution. More generally, these data also provide new evidence that BOLD response measured by fMRI do not precisely coincide with local electrophysiological activity (Logothetis, Pauls, Augath, Trinath, & Oeltermann, 2001; Niessing et al., 2005), and that different BOLD effects might possibly result from differences of just a few hundreds milliseconds in the time-course of neuronal responses. Further, our data indicate that significant amygdala activity might potentially take place and be evidenced by depth electrodes without a concomitant BOLD increase measured with fMRI, extending recent observation that BOLD and electrical activity might sometimes dissociate (Niessing et al., 2005).

These fMRI results may appear slightly discrepant at first sight with the fMRI results of Polli et al. (2008, 2009), as well as in light of the extant literature that primarily ascribed the detection or monitoring of negative events to the amygdala. Here, the patient SG showed larger amygdala responses to positive (hits), relative to negative events (errors), whereas an opposite effect was obtained in the fMRI studies of Polli et al. (2008, 2009). An interesting (although speculative at this stage) possibility is that errors would not be perceived as intense negative events in our task, whereas fast hits (which were overall very difficult to reach with the present task demands) would be perceived as definite positive events (even if

it remains at an implicit level, and the patients were not aware of this difference), creating a slight emotional imbalance between these two events (in favor of fast hits) with our speeded go/nogo task. This could potentially explain why the amygdala responded more strongly to fast hits than errors with this specific task. In the fMRI studies of Polli et al. (2008, 2009), perhaps a symmetric picture emerged, where errors were definitely perceived (and experienced) as negative events, whereas (more frequent and standard) correct responses were not processed as positive events by participants. As a result, the amygdala was responding more to errors than correct hits in these fMRI studies. Combined together (see Polli et al., 2008, 2009; and present fMRI results), these findings concur with the idea that the amygdala may be sensible to the behavioral relevance of motor actions, rather than their absolute valence (see Sander et al., 2003; Ousdal et al., 2008). Future studies should more directly manipulate this factor to test whether the amygdala is actually coding the behavioral relevance of motor actions, or another emotional dimension (such as the valence of motor actions).

Taken together, these results point to a specific involvement of the human amygdala in the rapid appraisal of performance during "simple" motor actions, beyond its well-established role in emotion or threat processing (see Davis & Whalen, 2001; Sander, Grafman, & Zalla, 2003; Zald, 2003; Whalen, 2007; Ousdal et al., 2008). These findings are consistent with models assuming that the amygdala may play a more general role in dynamically modulating the learning process of relevant associations between stimulus and response (see Sander et al., 2003; Phelps & LeDoux, 2005), thereby strengthening or reinforcing some advantageous stimulus-response mappings (fast hits), while conversely weakening some other erroneous associations (errors). Our study provides further evidence that the human amygdala plays such a key role in monitoring behavioral relevance of actions, in addition to (and in concert with) more cognitive or motoric functions subserved by the dorsal cingulate cortex (see also Polli et al., 2008, 2009).

Dorsal anterior cingulate and performance monitoring

By comparison, a clearly different neurophysiological profile was found in the left dorsal anterior cingulate gyrus (in patient SG). This region showed an early distinction between correct and incorrect responses that arose before motor execution, consistent with the notion that action monitoring in ACC may operate on internal signals from motor commands rather than external feedback (Holroyd et al., 2004). In addition, the critical dimension modulating ACC activity was the accuracy of action per se, but not its behavioral relevance or putative affective significance (see Ridderinkhof et al., 2007). Remarkably, correct rejections, which were not associated with any overt motor response, produced a similar neurophysiological signal compared to hits, while errors also differed from fast hits despite similar RTs. In other words, the distinctive signal to errors in dorsal cingulate did not reflect motor commands or actual motor execution per se, but the mismatch between intended and produced action, consistent with the internal monitoring function typically ascribed to ACC (Holroyd, Coles, & Nieuwenhuis, 2002; Ridderinkhof et al., 2007), and different from the motivational monitoring function presumably subserved by the amygdala. The fMRI results obtained for the dorsal cingulate cortex in the same patient further corroborate this conclusion, showing the strongest response to errors compared to all other conditions (hits and correct rejections).

In addition, in the cingulate, unlike the amygdala, we observed a significant linear relationship between the ERP component magnitude and speed of motor response (RTs), but specifically for slow hits. In this condition, the (peak) latency of the early cingulate positivity was inversely proportional to RT latency (i.e., the earlier this activity peaked relative to RTs, the slower the RTs), suggesting that this region might be closely related to motor preparation stages (see Holroyd & Coles, 2002; Ullsperger & von Cramon, 2003). This is consistent with the notion that dorsal ACC might receive direct inputs from motor commands in order to monitor ongoing actions or that it might participate to an early stage of motor preparation (Holroyd & Coles, 2002).

Although our intracranial results are broadly consistent with the notion that the dorsal ACC is primarily involved in performance monitoring, it must be emphasized that there have been several theoretical accounts or refinements put forward in the literature to account for the functions of the dorsal ACC (or more generally, the medial frontal cortex; see Ridderinkhof et al., 2007). Noteworthy, these alternative explanations might also provide plausible interpretations of our intracranial findings (for the dorsal ACC). For example, the medial frontal cortex may be involved in evaluating the reward of actions, estimating outcome values based on reinforcement history (using a cost-benefit analysis; see Rushworth, Buckley, Behrens, Walton, & Bannerman, 2007). Alternatively, the dorsal ACC could be involved in the suppression of externally triggered interfering programs (i.e. involved in overriding response; see Paus et al., 1991). Also plausible here, is the possibility that the ACC activity we recorded in this patient (SG) during the go/nogo task actually reflected response selection, rather than error monitoring per se (see Liu, Banich, Jacobson, & Tanabe, 2006). Consistent with this latter view, we found that the ACC activity arose before the motor response. Furthermore, the ACC (in concert with the dorsolateral prefrontal cortex) has been identified as an important structure for attentional control, in particular during response-related processes (Milham et al., 2001; Milham, Banich, Claus, & Cohen, 2003). Finally, it should also be pointed out that previous activation studies have typically found a more anterior (and/or superior) cingulate site involved in error/conflict monitoring (see e.g. Milham & Banich, 2005; Taylor et al., 2007), than the present location of the intracranial electrode (as well as the peak fMRI activation for errors) in patient SG.

The interpretation of the present intracranial findings should be viewed in light of some limitations. Because we recorded iLFPs from the left dorsal ACC (and left amygdala) of a single epileptic patient, a straightforward generalization of these statistical results to the (healthy) population was not feasible. Moreover, this patient (SG) had a clear epileptic history and accordingly, was treated with anti-epileptic drugs prior to our intracranial testing, which may have also affected normal brain functions. In addition, this patient (SG) had an atypical brain organization, characterized by the presence of periventricular heterotopias. This latter factor may also potentially explain why the fMRI peak activation for errors (relative to hits) was found to take place in a posterior cingulate cortex region, rather than a more anterior and medial frontal cortex area (e.g. dorsal ACC), as was consistently found across many previous activation studies performed in healthy volunteers during go/nogo tasks (see Simmonds, Pekar, & Mostofsky, 2008).

Conclusions

To conclude, our study sheds new lights on brain mechanisms underlying error detection, by showing an early involvement of the amygdala in action monitoring, but distinct from the role traditionally ascribed to ACC. This provides new support to some recent models of action monitoring (Polli et al., 2008, 2009), and may help explain discrepant findings concerning the exact role of the dorsal cingulate cortex in conflict and error monitoring (see Fellows & Farah, 2005). Here, by using intracranial recordings in two epileptic patients prior to surgery, we were able to demonstrate that the amygdala exhibited differential responses to correct actions and false alarms, mainly characterized by distinctive latencies around the time of actual motor response, and likely to contribute to appraising the affective significance (or salience) of motor actions. Amygdala activity was tightly coupled but clearly different from cingulate activity. These findings highlight that errors do not only recruit cognitive processes (reflected by activity in the cingulate), but also have an impact on brain systems involved in emotional processing and learning (as indexed by activity in the amygdala). Future studies should further examine the influence of such amygdala activity on autonomic arousal and learning induced by errors, and further investigate whether (and how) damage to the amygdala might impair the processing (or appraisal) of errors (see Fellows & Farah, 2005).

Acknowledgments

GP is supported by grants from the European Research Council (Starting Grant #200758) and Ghent University (BOF Grant #05Z01708). This work is supported by grants from the Swiss National Science Foundation (NCCR grant # 51A240-104897; Swiss National Centre for Competence in Research in Affective Sciences).

References

Brazdil, M., Roman, R., Falkenstein, M., Daniel, P., Jurak, P., & Rektor, I. (2002). Error processing--evidence from intracerebral ERP recordings. *Experimental Brain Research, 146*(4), 460-466.

Brodbeck, V., Lascano, A. M., Spinelli, L., Seeck, M., & Michel, C. M. (2009). Accuracy of EEG source imaging of epileptic spikes in patients with large brain lesions. *Clinical Neurophysiology, 120*(4), 679-685.

Brown, J. W., & Braver, T. S. (2005). Learned predictions of error likelihood in the anterior cingulate cortex. *Science, 307*(5712), 1118-1121.

Bush, G., Luu, P., & Posner, M. I. (2000). Cognitive and emotional influences in anterior cingulate cortex. *Trends in Cognitive Sciences, 4*(6), 215-222.

Carter, C. S., Braver, T. S., Barch, D. M., Botvinick, M. M., Noll, D., & Cohen, J. D. (1998). Anterior cingulate cortex, error detection, and the online monitoring of performance. *Science, 280*(5364), 747-749.

Cohen, M. X., & Ranganath, C. (2007). Reinforcement learning signals predict future decisions. *Journal of Neuroscience, 27*(2), 371-378.

Cohen, M. X., Ridderinkhof, K. R., Haupt, S., Elger, C. E., & Fell, J. (2008). Medial frontal cortex and response conflict: Evidence from human intracranial EEG and medial frontal cortex lesion. *Brain Research*.

Creutzfeldt, O. D., & Houchin, J. (1974). Neural basis of EEG waves. In A. Rémond (Ed.), *Handbook of electroencephalography and clinical neurophysiology* (Vol. IIC, pp. 5-55). Amsterdam: Elsevier.

Davis, M., & Whalen, P. J. (2001). The amygdala: vigilance and emotion. *Molecular Psychiatry, 6*(1), 13-34.

Debener, S., Ullsperger, M., Siegel, M., Fiehler, K., von Cramon, D. Y., & Engel, A. K. (2005). Trial-by-trial coupling of concurrent electroencephalogram and functional magnetic resonance imaging identifies the dynamics of performance monitoring. *Journal of Neuroscience, 25*(50), 11730-11737.

Dehaene, S., Posner, M. I., & Tucker, D. M. (1994). Localization of a neural system for error detection and compensation. *Psychological Science, 5*(5), 303-305.

Delorme, A., & Makeig, S. (2004). EEGLAB: an open source toolbox for analysis of single-trial EEG dynamics including independent component analysis. *Journal of Neuroscience Methods 134*, 9-21.

Essl, M., & Rappelsberger, P. (1998). EEG coherence and reference signals: experimental results and mathematical explanations. *Medical and Biological Engineering and Computing, 36*(4), 399-406.

Fales, C. L., Barch, D. M., Rundle, M. M., Mintun, M. A., Snyder, A. Z., Cohen, J. D., et al. (2008). Altered emotional interference processing in affective and cognitive-control brain circuitry in major depression. *Biological Psychiatry, 63*(4), 377-384.

Falkenstein, M., Hoormann, J., Christ, S., & Hohnsbein, J. (2000). ERP components on reaction errors and their functional significance: a tutorial. *Biological Psychology, 51*(2-3), 87-107.

Fellows, L. K., & Farah, M. J. (2005). Is anterior cingulate cortex necessary for cognitive control? *Brain, 128*(Pt 4), 788-796.

Frank, M. J., Woroch, B. S., & Curran, T. (2005). Error-related negativity predicts reinforcement learning and conflict biases. Neuron, 47(4), 495-501.

Friston, K. J., Fletcher, P., Josephs, O., Holmes, A., Rugg, M. D., & Turner, R. (1998). Event-related fMRI: characterizing differential responses. *Neuroimage, 7*(1), 30-40.

Garavan, H., Ross, T. J., Murphy, K., Roche, R. A., & Stein, E. A. (2002). Dissociable executive functions in the dynamic control of behavior: inhibition, error detection, and correction. *Neuroimage, 17*(4), 1820-1829.

Gehring, W. J., & Fencsik, D. E. (2001). Functions of the medial frontal cortex in the processing of conflict and errors. *Journal of Neuroscience, 21*(23), 9430-9437.

Gehring, W. J., Goss, B., Coles, M. G., Meyer, D. E., & Donchin, E. (1993). A neural system for error detection and compensation. *Psychological Science, 4*, 385–390.
Gratton, G., Coles, M. G. H., & Donchin, E. (1992). Optimizing the Use of Information - Strategic Control of Activation of Responses. *Journal of Experimental Psychology-General, 121*(4), 480-506.
Hajcak, G., & Foti, D. (2008). Errors are aversive: defensive motivation and the error-related negativity. *Psychological Science, 19*(2), 103-108.
Hajcak, G., McDonald, N., & Simons, R. F. (2003a). Anxiety and error-related brain activity. *Biological Psychology, 64*(1-2), 77-90.
Hajcak, G., McDonald, N., & Simons, R. F. (2003b). To err is autonomic: error-related brain potentials, ANS activity, and post-error compensatory behavior. *Psychophysiology, 40*(6), 895-903.
Hajcak, G., McDonald, N., & Simons, R. F. (2004). Error-related psychophysiology and negative affect. *Brain and Cognition, 56*(2), 189-197.
Hajcak, G., Moser, J. S., Yeung, N., & Simons, R. F. (2005). On the ERN and the significance of errors. *Psychophysiology, 42*(2), 151-160.
Holroyd, C. B., & Coles, M. G. (2002). The neural basis of human error processing: reinforcement learning, dopamine, and the error-related negativity. *Psychological Review, 109*(4), 679-709.
Holroyd, C. B., Coles, M. G., & Nieuwenhuis, S. (2002). Medial prefrontal cortex and error potentials. *Science, 296*(5573), 1610-1611 author reply 1610-1611.
Holroyd, C. B., Nieuwenhuis, S., Yeung, N., Nystrom, L., Mars, R. B., Coles, M. G., et al. (2004). Dorsal anterior cingulate cortex shows fMRI response to internal and external error signals. *Nature Neuroscience, 7*(5), 497-498.
Kienast, T., Hariri, A. R., Schlagenhauf, F., Wrase, J., Sterzer, P., Buchholz, H. G., et al. (2008). Dopamine in amygdala gates limbic processing of aversive stimuli in humans. *Nature Neuroscience*.
Laming, D. (1968). *Information theory of choice-reaction times*. London: Academic Press.
Lang, P. J., Bradley, M. M., & Cuthbert, B. N. (1990). Emotion, attention, and the startle reflex. *Psychological Review, 97*(3), 377-395.
Li, C. S., Yan, P., Chao, H. H., Sinha, R., Paliwal, P., Constable, R. T., et al. (2008). Error-specific medial cortical and subcortical activity during the stop signal task: a functional magnetic resonance imaging study. *Neuroscience, 155*(4), 1142-1151.
Liu, X., Banich, M. T., Jacobson, B. L., & Tanabe, J. L. (2006). Functional dissociation of attentional selection within PFC: response and non-response related aspects of attentional selection as ascertained by fMRI. *Cerebral Cortex*, 16(6), 827-834.
Logothetis, N. K., Pauls, J., Augath, M., Trinath, T., & Oeltermann, A. (2001). Neurophysiological investigation of the basis of the fMRI signal. *Nature, 412*(6843), 150-157.
Luu, P., Flaisch, T., & Tucker, D. M. (2000). Medial frontal cortex in action monitoring. Journal of Neuroscience, 20(1), 464-469.
Luu, P., Tucker, D. M., Derryberry, D., Reed, M., & Poulsen, C. (2003). Electrophysiological responses to errors and feedback in the process of action regulation. *Psychological Science, 14*(1), 47-53.
Luu, P., Tucker, D. M., & Makeig, S. (2004). Frontal midline theta and the error-related negativity: neurophysiological mechanisms of action regulation. *Clinical Neurophysiology, 115*(8), 1821-1835.
Makeig, S. (1993). Auditory Event-Related Dynamics of the EEG Spectrum and Effects of Exposure to Tones *Electroencephalography and Clinical Neurophysiology, 86*, 283-293.
Manly, B. F. (1991). *Randomization and Monte Carlo Methods in Biology*. London, UK: Chapman & Hall.

Menon, V., Adleman, N. E., White, C. D., Glover, G. H., & Reiss, A. L. (2001). Error-related brain activation during a Go/NoGo response inhibition task. *Human Brain Mapping, 12*(3), 131-143.

Milham, M. P., & Banich, M. T. (2005). Anterior cingulate cortex: an fMRI analysis of conflict specificity and functional differentiation. *Human Brain Mapping*, 25(3), 328-335.

Milham, M. P., Banich, M. T., Claus, E. D., & Cohen, N. J. (2003). Practice-related effects demonstrate complementary roles of anterior cingulate and prefrontal cortices in attentional control. *Neuroimage*, 18(2), 483-493.

Milham, M. P., Banich, M. T., Webb, A., Barad, V., Cohen, N. J., Wszalek, T., et al. (2001). The relative involvement of anterior cingulate and prefrontal cortex in attentional control depends on nature of conflict. *Brain Research Cognitive Brain Research*, 12(3), 467-473.

Niedermeyer, E., & Lopes da Silva, F. (2004). *Electroencephalography: Basic Principles, Clinical Applications, and Related Fields*: Lippincott Williams & Wilkins.

Niessing, J., Ebisch, B., Schmidt, K. E., Niessing, M., Singer, W., & Galuske, R. A. (2005). Hemodynamic signals correlate tightly with synchronized gamma oscillations. *Science, 309*(5736), 948-951.

Ochsner, K. N., & Gross, J. J. (2005). The cognitive control of emotion. *Trends in Cognitive Sciences, 9*(5), 242-249.

Ongur, D., & Price, J. L. (2000). The organization of networks within the orbital and medial prefrontal cortex of rats, monkeys and humans. *Cerebral Cortex, 10*(3), 206-219.

Ousdal, O. T., Jensen, J., Server, A., Hariri, A. R., Nakstad, P. H., & Andreassen, O. A. (2008). The human amygdala is involved in general behavioral relevance detection: evidence from an event-related functional magnetic resonance imaging Go-NoGo task. *Neuroscience*, 156(3), 450-455.

Parkes, L. M., Bastiaansen, M. C., & Norris, D. G. (2006). Combining EEG and fMRI to investigate the post-movement beta rebound. Neuroimage, 29(3), 685-696.

Paus, T., Kalina, M., Patockova, L., Angerova, Y., Cerny, R., Mecir, P., et al. (1991). Medial vs lateral frontal lobe lesions and differential impairment of central-gaze fixation maintenance in man. *Brain*, 114 (Pt 5), 2051-2067.

Phelps, E. A., & LeDoux, J. E. (2005). Contributions of the amygdala to emotion processing: from animal models to human behavior. *Neuron, 48*(2), 175-187.

Pizzagalli, D. A., Peccoralo, L. A., Davidson, R. J., & Cohen, J. D. (2006). Resting anterior cingulate activity and abnormal responses to errors in subjects with elevated depressive symptoms: a 128-channel EEG study. *Human Brain Mapping, 27*(3), 185-201.

Polli, F. E., Barton, J. J., Thakkar, K. N., Greve, D. N., Goff, D. C., Rauch, S. L., et al. (2008). Reduced error-related activation in two anterior cingulate circuits is related to impaired performance in schizophrenia. *Brain, 131*(Pt 4), 971-986.

Polli, F.E., Wright, C.I., Milad, M.R., Dickerson, B.C., Vangel, M., Barton, J.J., Rauch, S.L., & Manoach, D.S. (2009). Hemispheric differences in amygdala contributions to response monitoring. *Neuroreport*, 20(4), 398-402.

Pourtois, G., Peelen, M. V., Spinelli, L., Seeck, M., & Vuilleumier, P. (2007). Direct intracranial recording of body-selective responses in human extrastriate visual cortex. *Neuropsychologia, 45*(11), 2621-2625.

Rabbitt, P. M. (1966). Errors and error correction in choice-response tasks. *Journal of Experimental Psychology, 71*(2), 264-272.

Rappelsberger, P., Pfurtscheller, G., & Filz, O. (1994). Calculation of event-related coherence--a new method to study short-lasting coupling between brain areas. *Brain Topography, 7*(2), 121-127.

Ridderinkhof, K. R., Nieuwenhuis, S., & Braver, T. S. (2007). Medial frontal cortex function: an introduction and overview. *Cognitive, Affective & Behavioral Neuroscience, 7*(4), 261-265.

Ridderinkhof, K. R., Ullsperger, M., Crone, E. A., & Nieuwenhuis, S. (2004). The role of the medial frontal cortex in cognitive control. *Science, 306*(5695), 443-447.

Ridderinkhof, K. R., van den Wildenberg, W. P., Segalowitz, S. J., & Carter, C. S. (2004). Neurocognitive mechanisms of cognitive control: the role of prefrontal cortex in action selection, response inhibition, performance monitoring, and reward-based learning. *Brain and Cognition, 56*(2), 129-140.

Rushworth, M. F., Buckley, M. J., Behrens, T. E., Walton, M. E., & Bannerman, D. M. (2007). Functional organization of the medial frontal cortex. *Current Opinion in Neurobiology*, 17(2), 220-227.

Sander, D., Grafman, J., & Zalla, T. (2003). The human amygdala: an evolved system for relevance detection. *Reviews in the Neurosciences, 14*(4), 303-316.

Seeck, M., & Spinelli, L. (2004). Intracranial monitoring. *Clinical Neurophysiology, 57*, 485-493.

Simmonds, D. J., Pekar, J. J., & Mostofsky, S. H. (2008). Meta-analysis of Go/No-go tasks demonstrating that fMRI activation associated with response inhibition is task-dependent. *Neuropsychologia*, 46(1), 224-232.

Stevens, M. C., Kiehl, K. A., Pearlson, G. D., & Calhoun, V. D. (2007). Brain network dynamics during error commission. *Human Brain Mapping*.

Swick, D., & Turken, A. U. (2002). Dissociation between conflict detection and error monitoring in the human anterior cingulate cortex. *Proceedings of the National Academy of Sciences of the United States of America, 99*(25), 16354-16359.

Taylor, S. F., Martis, B., Fitzgerald, K. D., Welsh, R. C., Abelson, J. L., Liberzon, I., et al. (2006). Medial frontal cortex activity and loss-related responses to errors. *Journal of Neuroscience, 26*(15), 4063-4070.

Taylor, S. F., Stern, E. R., & Gehring, W. J. (2007). Neural systems for error monitoring: recent findings and theoretical perspectives. *Neuroscientist, 13*(2), 160-172.

Ullsperger, M., & von Cramon, D. Y. (2001). Subprocesses of performance monitoring: a dissociation of error processing and response competition revealed by event-related fMRI and ERPs. *Neuroimage, 14*(6), 1387-1401.

Ullsperger, M., & von Cramon, D. Y. (2003). Error monitoring using external feedback: specific roles of the habenular complex, the reward system, and the cingulate motor area revealed by functional magnetic resonance imaging. *Journal of Neuroscience, 23*(10), 4308-4314.

Ullsperger, M., & von Cramon, D. Y. (2004). Neuroimaging of performance monitoring: error detection and beyond. *Cortex, 40*(4-5), 593-604.

van Hoesen, G. W., Morecraft, R. J., & Vogt, B. A. (1993). Connections of the monkey cingulate cortex. In B. A. Vogt & M. Gabriel (Eds.), *Neurobiology of cingulate cortex and limbic thalamus: a comprehensive handbook* (pp. 249-284). Boston: : Birkhauser.

Van Veen, V., & Carter, C. S. (2002). The timing of action-monitoring processes in the anterior cingulate cortex. *Journal of Cognitive Neuroscience, 14*(4), 593-602.

van Veen, V., & Carter, C. S. (2006). Error detection, correction, and prevention in the brain: a brief review of data and theories. *Clinical EEG & Neuroscience, 37*(4), 330-335.

Vocat, R., Pourtois, G., & Vuilleumier, P. (2008). Unavoidable errors: a spatio-temporal analysis of time-course and neural sources of evoked potentials associated with error processing in a speeded task. *Neuropsychologia, 46*(10), 2545-2555.

Wang, C., Ulbert, I., Schomer, D. L., Marinkovic, K., & Halgren, E. (2005). Responses of human anterior cingulate cortex microdomains to error detection, conflict monitoring, stimulus-response mapping, familiarity, and orienting. *Journal of Neuroscience, 25*(3), 604-613.

Whalen, P. J. (2007). The uncertainty of it all. *Trends in Cognitive Sciences, 11*(12), 499-500.

Zald, D. H. (2003). The human amygdala and the emotional evaluation of sensory stimuli. *Brain Research Brain Research Review, 41*(1), 88-123.

Figures legends

Figure 1. Sites of intracranial electrodes in patient SG, corresponding **(A)** to the depth of the left dorsal cingulate gyrus, as evidenced using a sagittal view (Talairach coordinates: -25x, -8y, +38z), **(B)** left amygdala (-29x, -10y, -15z), and **(C)** left anterior hippocampus (-25x, -18y, -17z). Sites of intracranial electrodes in patient VM corresponding to **(D)** the right amygdala (25x, -4y, -27z) and **(E)** right anterior hippocampus (26x, -16y, -24z).

Figure 2. Behavioral results of the two patients as compared with a group of 16 healthy participants (see Vocat et al., 2008). **(A)** Accuracy and **(B)** mean RTs in the different conditions. The two patients showed the same pattern as healthy participants. Importantly, RTs were similar for errors (false alarms) and fast hits. A systematic post-error slowing (N-1) was also found in all participants, confirming normal monitoring and adjustment.

Figure 3. Intracranial ERP results in patient SG for the left dorsal cingulate gyrus (**A,B**) and left amygdala (**C,D**). ERP data were epoched from the onset of the imperative stimulus (**A,C**) or from motor response (**B,D**); note that no response was made on correct rejections (successful inhibitions). In both brain regions, a conspicuous response-related (as opposed to stimulus-related) activity was recorded, though with very different profiles for the cingulate vs. amygdala. The cingulate showed an extra positive ERP starting just before motor response, probably reflecting error detection per se, while the amygdala showed a distinct temporal pattern as a function of accuracy (fast hits vs. errors) and uncertainty (fast vs. slow hits). See text for numerical results and statistical tests.

Figure 4. Trial by trial breakdown of iLFPs (ERP images, see Delorme & Makeig, 2004) for each condition and each region separately, in patient SG. Reliable responses were found around motor execution at the single-trial level for the left dorsal cingulate (**A:** slow hits, **B:** fast hits and **C:** errors) and the left amygdala **(D:** slow hits, **E:** fast hits and **F:** errors). These analyses rule out the possibility of residual epileptic/spiking activity or progressive changes accounting for differences between regions or between conditions. In the cingulate, errors (**C**) were clearly distinct from both slow hits (**A**) and fast hits (**B**), characterized by an extra positivity around motor execution and a delayed sustained negativity. By contrast, the left amygdala showed an ample positive ERP component that was systematically delayed for errors **(F)** compared to fast hits (**E**) and slow hits (**D**).

Figure 5. (**A**) Polarity reversal for iLFPs recorded in the left amygdala and left anterior hippocampus in SG (fast hits condition), suggesting a local neural generator. The reversal was not complete, as the response peak was slightly earlier in the amygdala than the hippocampus. (**B,C,D,E**) Trial by trial breakdown (fast hits condition) for electrodes located in the left anterior hippocampus (**B**), in the left amygdala (Talairach coordinates: -29x, -10y, -

15z) (**C**); in a more lateral site nearby the amygdala (peri-amygdala region; -39x, -8y, -17z) (**D**), and more remotely in the left lateral temporal lobe (-52x, -6y, -19z) (**E**). These data (**C,D,E**) clearly show an amplitude gradient with maximum amplitude in the left amygdala region.

Figure 6. ERPs as a function of motor response speed. (**A**) A clear inverse relationship was found between the early positive activity in dorsal cingulate and RTs for the slow hits condition. The earlier the positivity peak relative to RTs, the slower RTs. (**B**) This inverse correlation in the slow hits condition was further evidenced when computing an ERP image with individual trials sorted from the fastest to the slowest RT. The black dashed line (after response) represents the RT distribution, from the fastest (bottom) to the slowest (top). The gray dashed line (before response) shows the peak of the positive ERP activity prior to response onset. This correlation was not seen for fast hits (**D**) or errors (**E**) in the cingulate, and not found in the amygdala for either condition, including slow hits **(C)**.

Figure 7. Time-frequency decompositions of single trial data for each condition and each region separately in patient SG. (**A,B,C**) In the left cingulate, a first transient spectral change arose in the theta band (increase) just prior to motor execution, followed by two more sustained changes in the alpha (decrease) and beta (increase) band. This later increase in beta amplitude was not seen following errors (**C**), but only after the slow (**A**) or fast hits (**B**). In the left amygdala (**D,E,F**), the spectral content of intracranial ERPs showed a different pattern of event-related modulations, with a reliable theta increase around motor execution after slow (**D**) and fast hits (**E**), which was much more delayed (and now twofold) after errors (**F**). A coherence analysis between the left cingulate and left amygdala was also performed for each condition separately (**G,H,I**), and revealed a reliable increase in coherence between these two regions, mainly arising in the theta band and selectively delayed for errors (**I**) relative either to slow hits (**G**) or fast hits (**H**).

Figure 8. Intracranial ERP results from the right amygdala in patient VM. (**A**) Similarly to the left amygdala (patient SG), a clear monophasic ERP response arose around motor execution, but its latency was delayed by 250 ms for errors relative to fast hits, despite the lack of substantial RT differences between these two conditions, replicating the pattern found for the left amygdala in patient SG (see Fig. 3). (**B**) Polarity reversal was observed between the right amygdala and adjacent right anterior hippocampus, confirming the existence of local neural generators. **(C,D,E)** Trial-by-trial breakdown (ERP image) of data from each condition in the right amygdala showed that the positive ERP component could be reliably detected even at the single trial level in the fast hits (**D**) and errors (**E**) conditions, with a systematic delay in the latter compared to the former case. A positive ERP response was not detected around motor execution in the slow hits conditions (**C**), but only a late response to the visual feedback.

Figure 9. Main fMRI results in patient SG. (**A**) Bilateral activation (p<.001 uncorrected) to errors, relative to fast hits, in the dorsal cingulate cortex. (**B**) Parameter estimates from the cingulate peaks confirmed greater responses to commission errors, relative to other conditions, consistent with a key role in detecting action error. (**C**) Bilateral activation (p<.001 uncorrected) to fast hits, relative to errors, in the amygdala. (**D**) Parameter estimates from amygdala peaks confirmed greater responses when outcome was positive (i.e. correct fast hits or correct rejections), consistent with a role in monitoring action success. (**B,D**) For each condition, parameter estimates were subtracted from the control baseline condition (see methods).

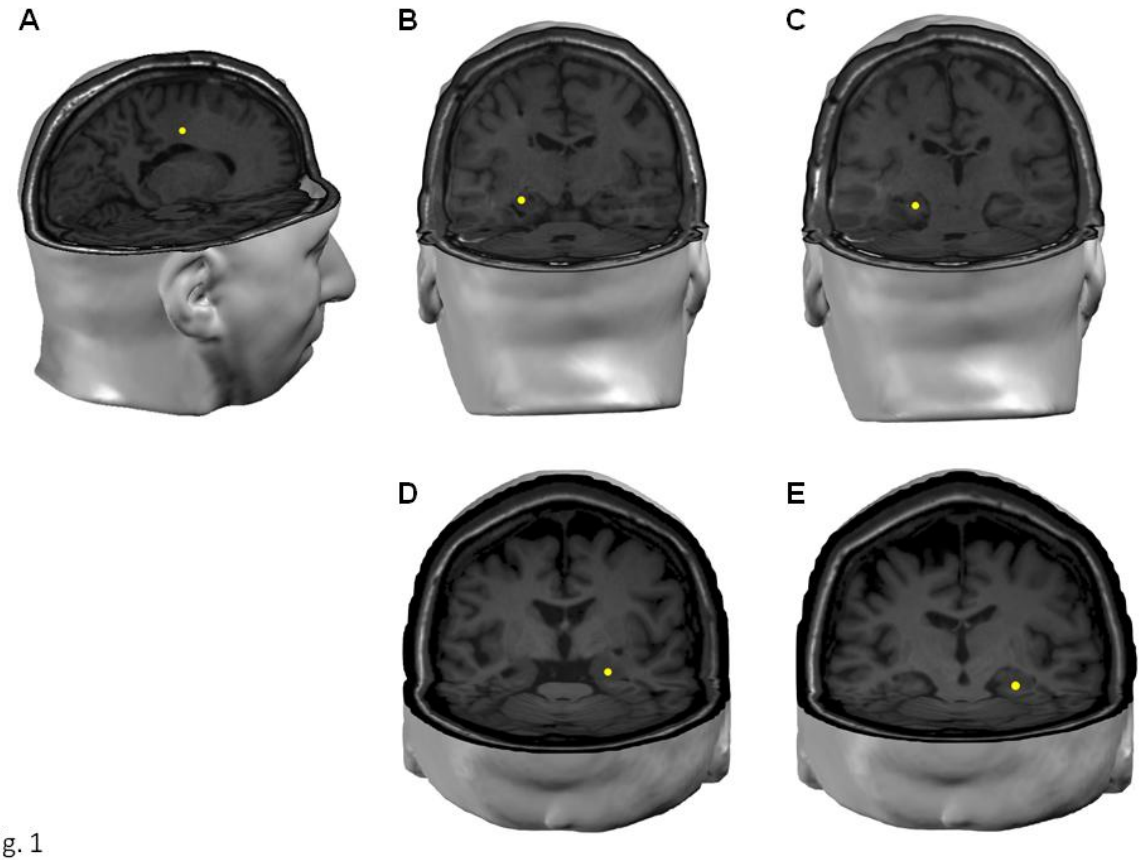

Fig. 1

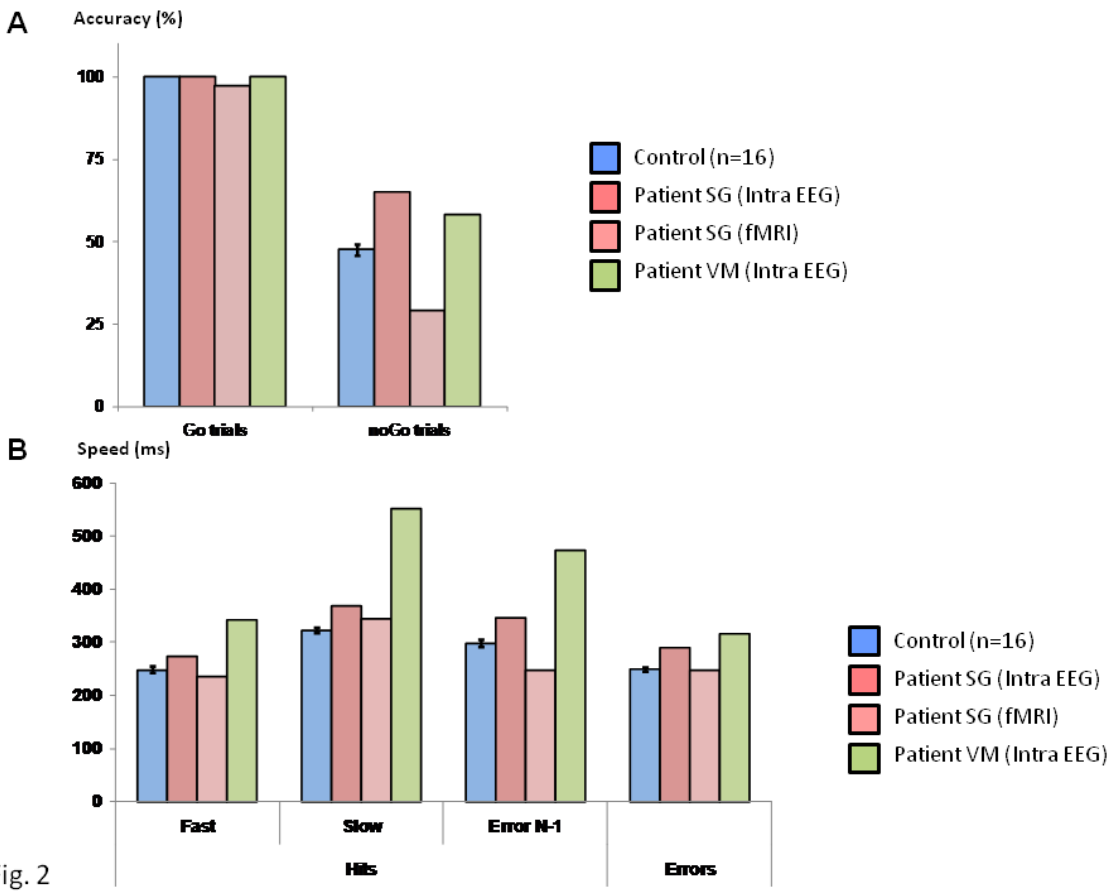
A
Accuracy (%)
100
75
50
25
0
Go trials
noGo trials
Control (n=16)
Patient SG (Intra EEG)
Patient SG (fMRI)
Patient VM (Intra EEG)
B
Speed (ms)
600
500
400
300
200
100
0
Fast
Slow
Error N-1
Hits
Errors
Control (n=16)
Patient SG (Intra EEG)
Patient SG (fMRI)
Patient VM (Intra EEG)

Fig. 2

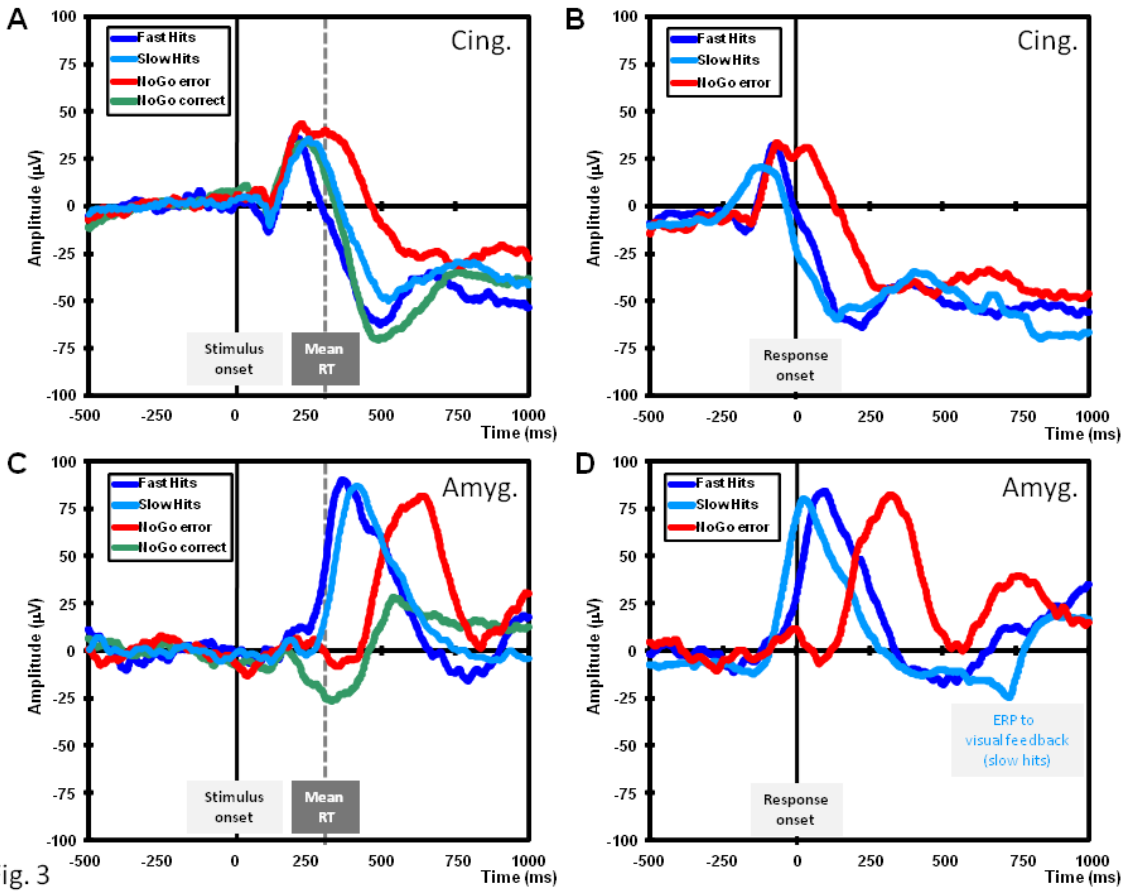
A
Cing.
Fast Hits
Slow Hits
NoGo error
NoGo correct
Amplitude (μV)
Stimulus onset
Mean RT
Time (ms)
B
Cing.
Fast Hits
Slow Hits
NoGo error
Response onset
Time (ms)
C
Amyg.
Fast Hits
Slow Hits
NoGo error
NoGo correct
Stimulus onset
Mean RT
Time (ms)
D
Amyg.
Fast Hits
Slow Hits
NoGo error
ERP to visual feedback (slow hits)
Response onset
Time (ms)

Fig. 3

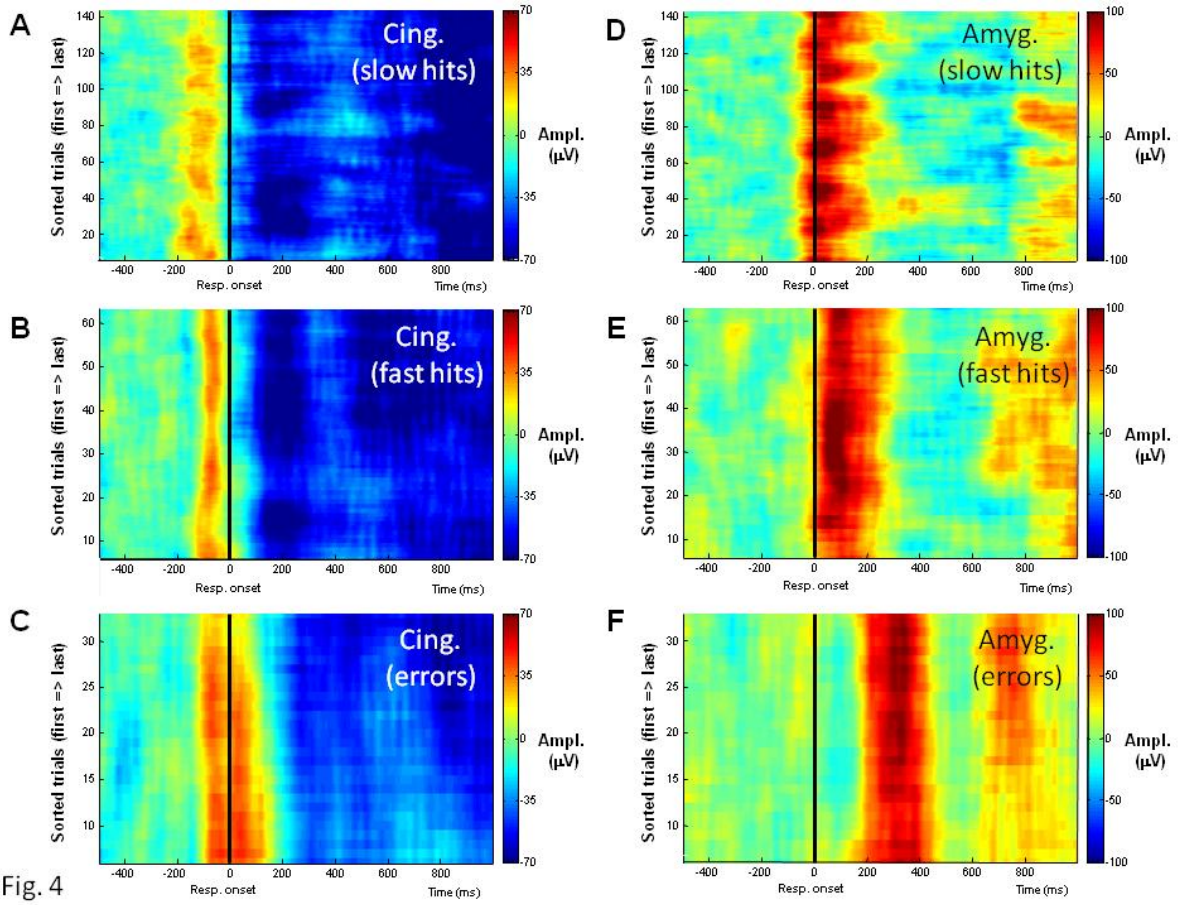
A
Cing.
(slow hits)
B
Cing.
(fast hits)
C
Cing.
(errors)
D
Amyg.
(slow hits)
E
Amyg.
(fast hits)
F
Amyg.
(errors)
Sorted trials (first => last)
Resp. onset
Time (ms)
Ampl.
(µV)

Fig. 4

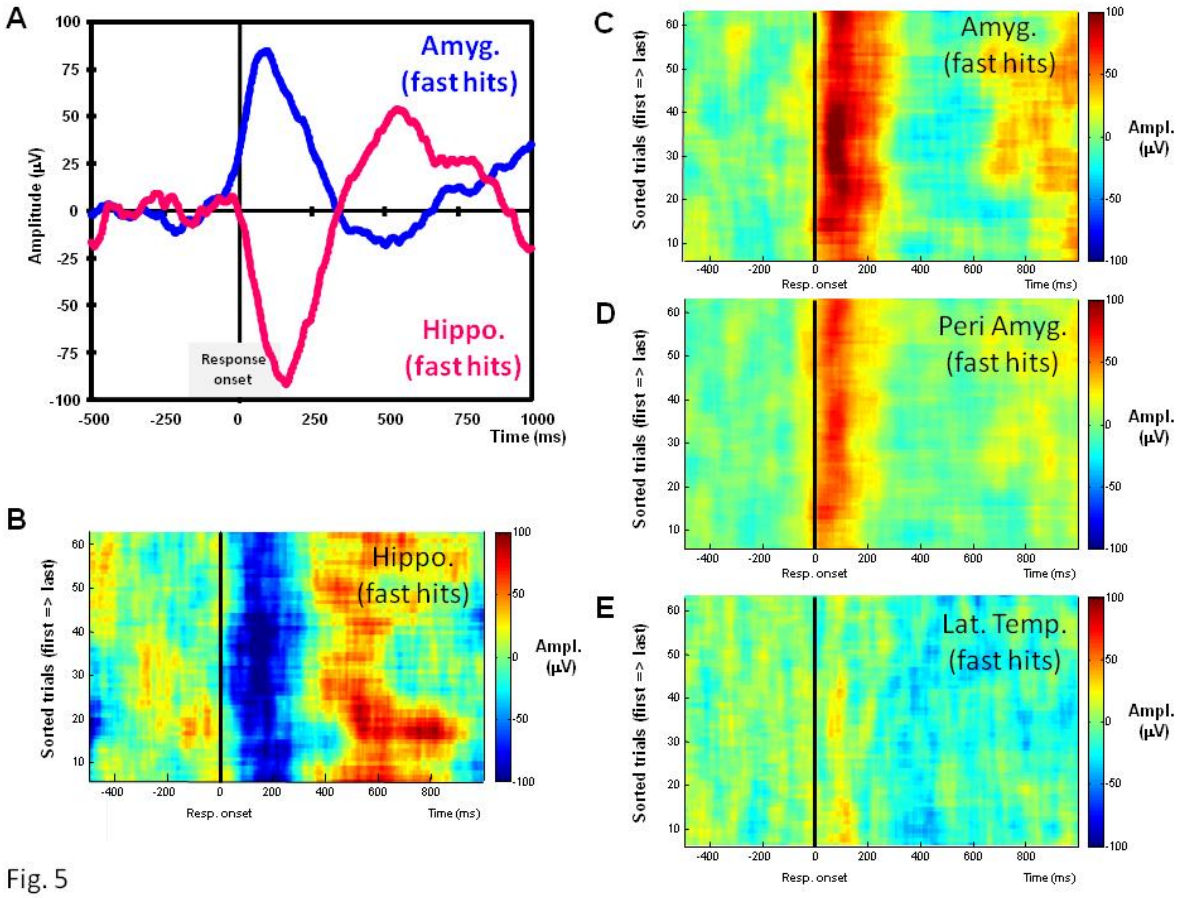
A
Amyg.
(fast hits)
Hippo.
(fast hits)
Response
onset
Amplitude (µV)
Time (ms)
B
Hippo.
(fast hits)
Sorted trials (first => last)
Resp. onset
Time (ms)
Ampl.
(µV)
C
Amyg.
(fast hits)
D
Peri Amyg.
(fast hits)
E
Lat. Temp.
(fast hits)

Fig. 5

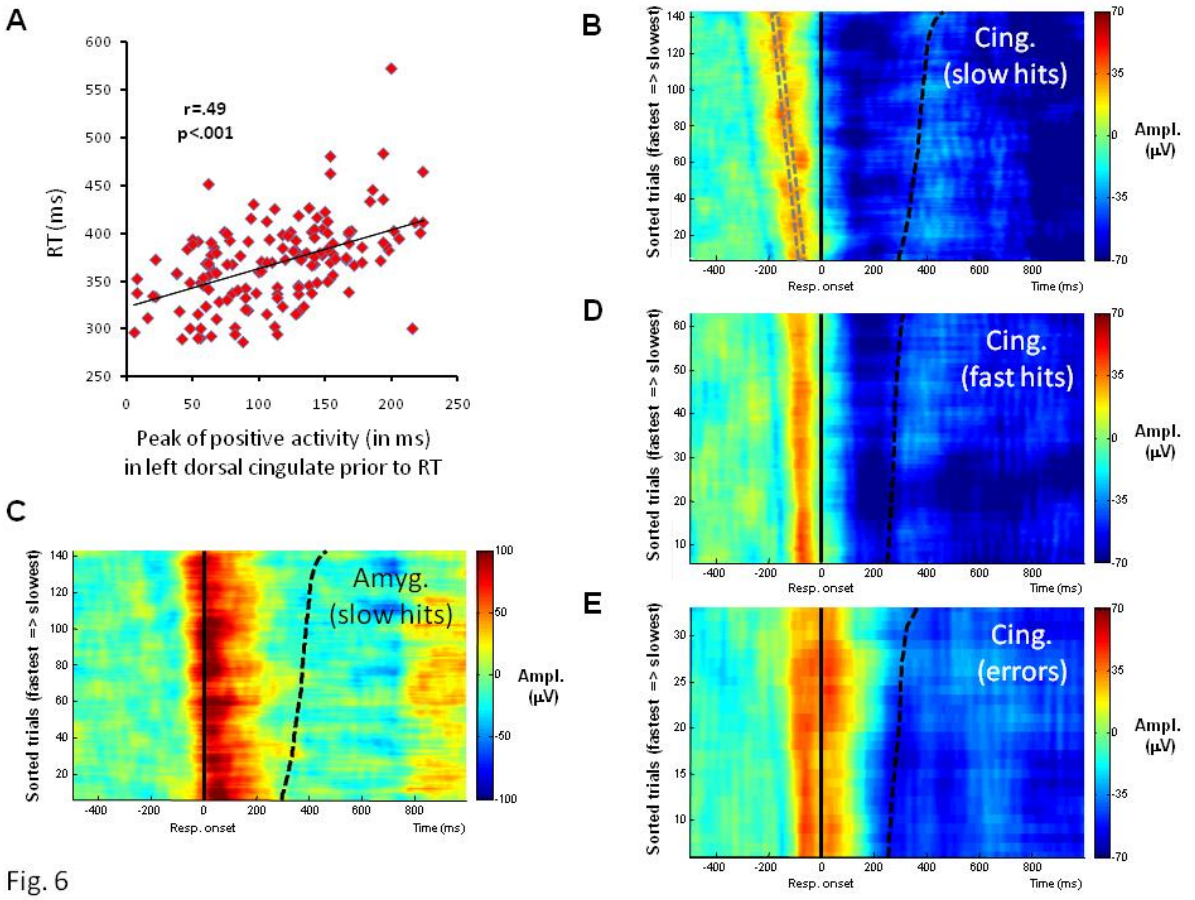
A
r=.49
p<.001
RT (ms)
Peak of positive activity (in ms)
in left dorsal cingulate prior to RT
B
Cing.
(slow hits)
D
Cing.
(fast hits)
E
Cing.
(errors)
C
Amyg.
(slow hits)
Sorted trials (fastest => slowest)
Resp. onset
Time (ms)
Ampl.
(μV)

Fig. 6

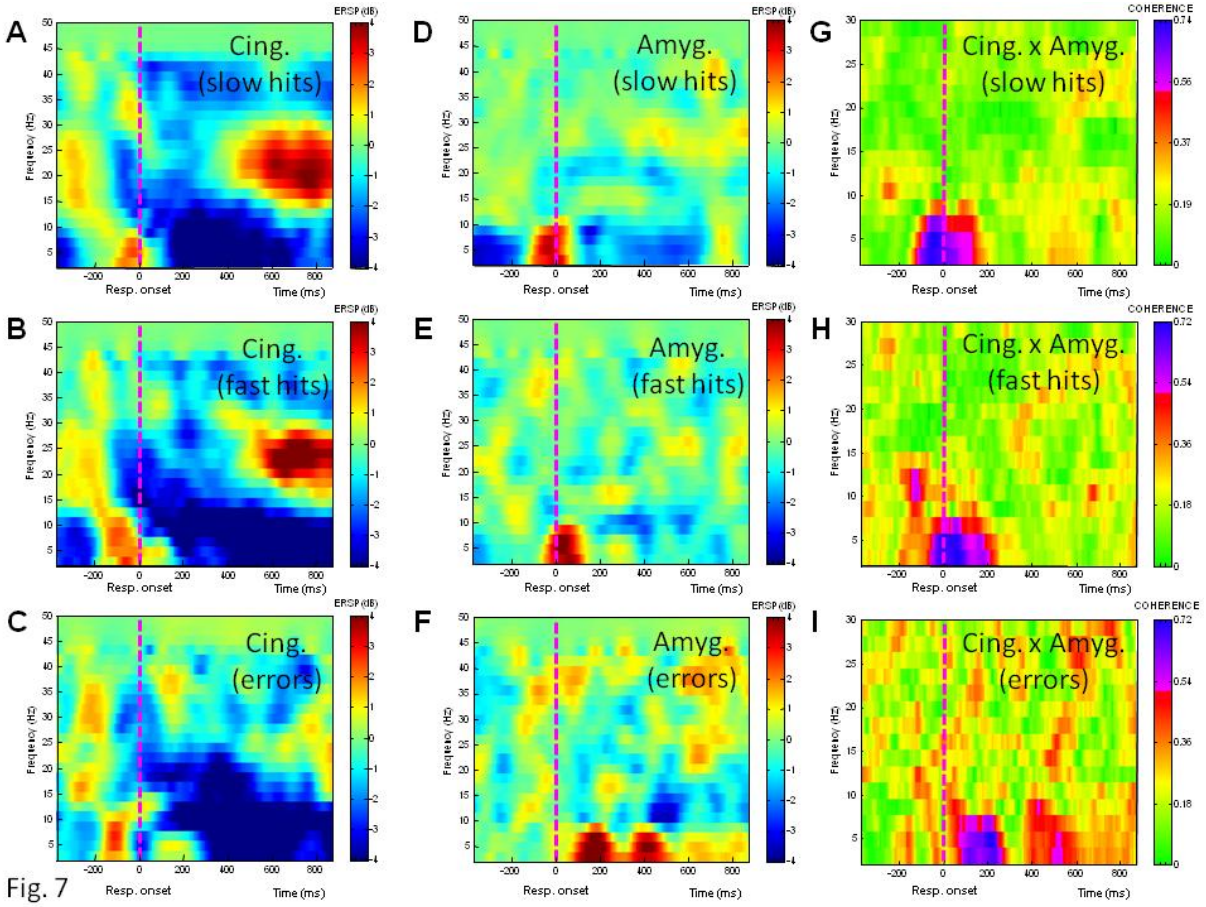
A
Cing.
(slow hits)
B
Cing.
(fast hits)
C
Cing.
(errors)
D
Amyg.
(slow hits)
E
Amyg.
(fast hits)
F
Amyg.
(errors)
G
Cing. x Amyg.
(slow hits)
H
Cing. x Amyg.
(fast hits)
I
Cing. x Amyg.
(errors)
ERSP (dB)
COHERENCE
Frequency (Hz)
Resp. onset
Time (ms)

Fig. 7

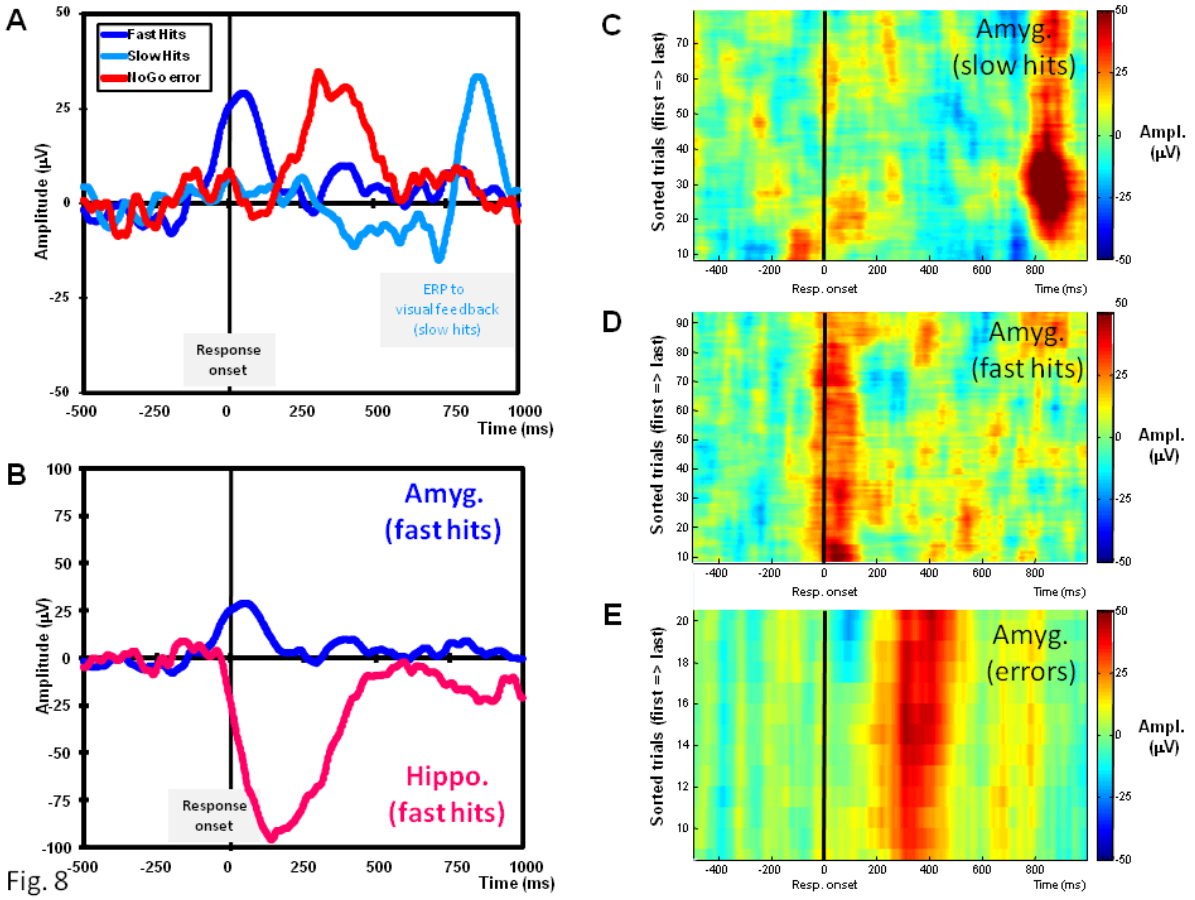
A
Fast Hits
Slow Hits
NoGo error
Amplitude (µV)
Response onset
ERP to visual feedback (slow hits)
Time (ms)
B
Amyg. (fast hits)
Hippo. (fast hits)
Response onset
Amplitude (µV)
Time (ms)
C
Amyg. (slow hits)
Sorted trials (first => last)
Resp. onset
Time (ms)
Ampl. (µV)
D
Amyg. (fast hits)
Sorted trials (first => last)
Resp. onset
Time (ms)
Ampl. (µV)
E
Amyg. (errors)
Sorted trials (first => last)
Resp. onset
Time (ms)
Ampl. (µV)

Fig. 8

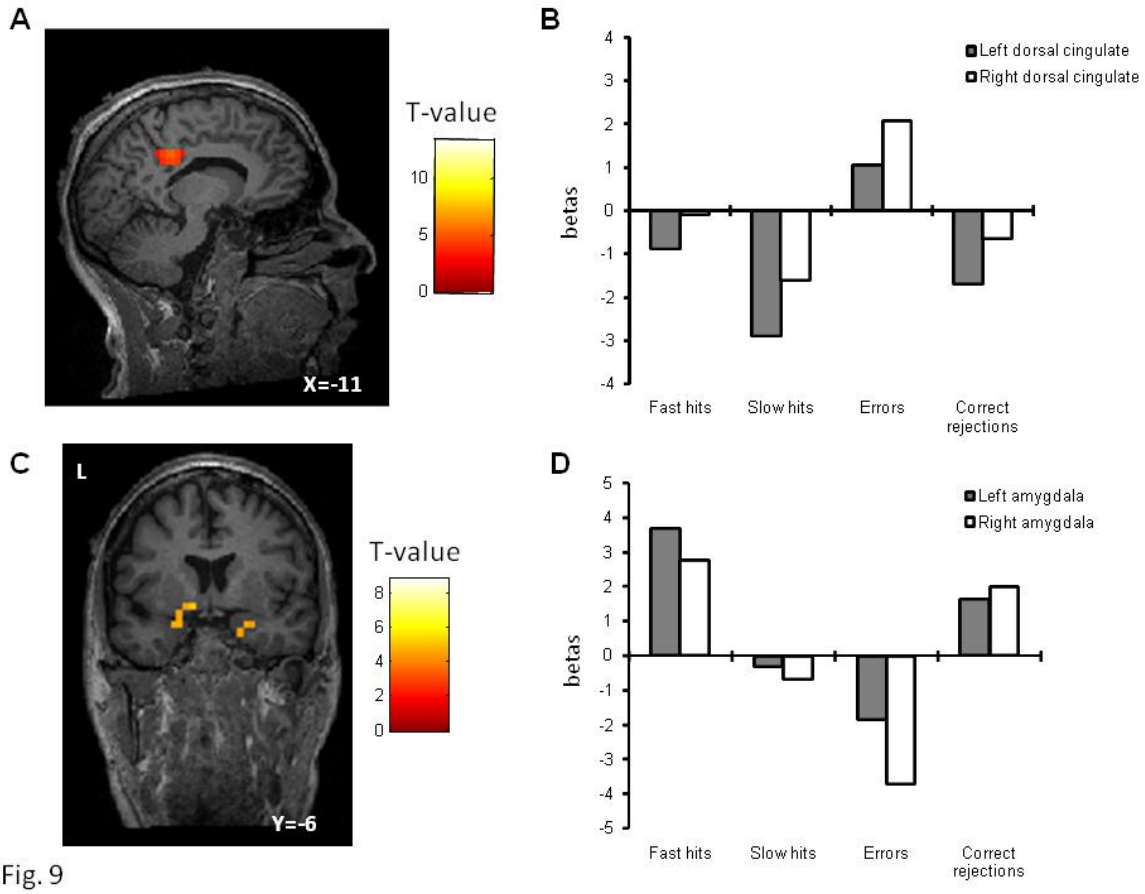
A
X=-11
T-value
10
5
0
B
Left dorsal cingulate
Right dorsal cingulate
betas
4
3
2
1
0
-1
-2
-3
-4
Fast hits
Slow hits
Errors
Correct rejections
C
L
Y=-6
T-value
8
6
4
2
0
D
Left amygdala
Right amygdala
betas
5
4
3
2
1
0
-1
-2
-3
-4
-5
Fast hits
Slow hits
Errors
Correct rejections

Fig. 9